

Exploring Plasma Dynamics with Laboratory Magnetospheres

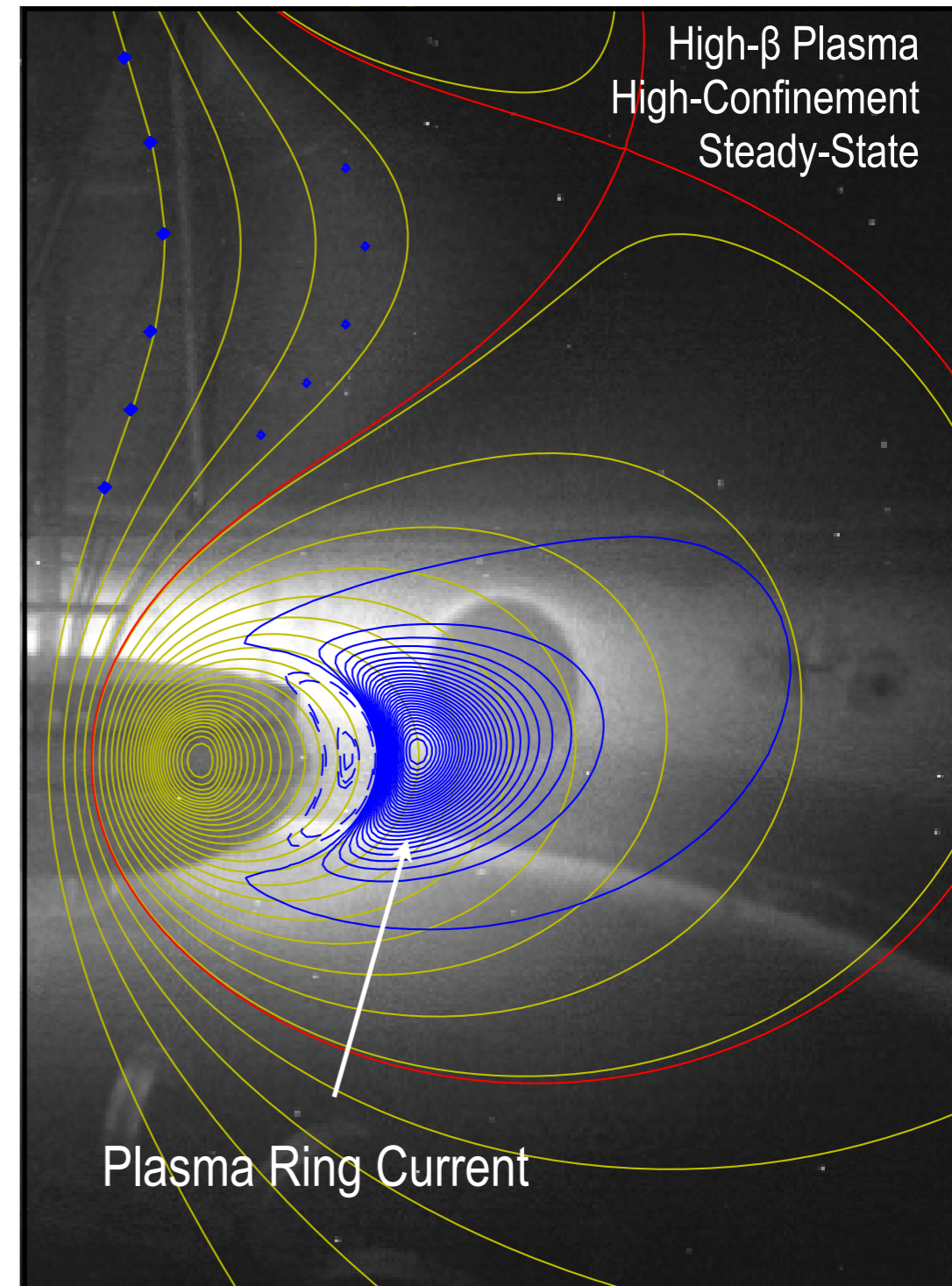
Mike Mauel and
LDX and CTX Experimental Teams
Columbia University and PSFC, MIT

Michigan Institute for Plasma Science and Engineering
February 2014

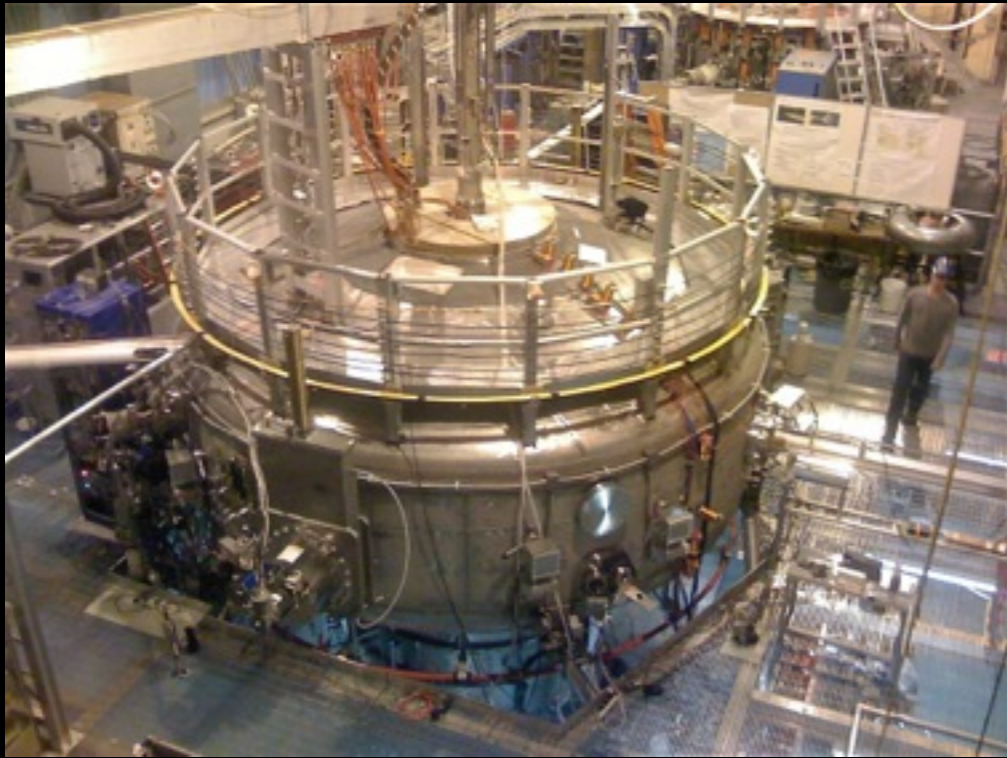


Laboratory Magnetospheres are facilities for study of steady-state and high-beta plasma transport and can test space physics and technology in relevant magnetic geometry

- Very high plasma pressure, $\beta > 50\%$, when dipole is magnetically levitated **showing key connection between laboratory and planetary magnetospheres**
- Very strong, but small, dipole magnet inside a very large vacuum chamber **making possible very large plasma experiments at relatively low cost**
- Electron cyclotron waves (“chorus”, ECH) and radio waves (Alfvén and ion-cyclotron waves) heat and maintain plasma and trapped particles **giving variety and control over plasma properties**
- Whole plasma access for **unparalleled imaging and diagnostic measurement**
- Polar boundary control and polar diagnostics **when dipole is mechanically supported**



Laboratory Magnetospheres: Facilities for Controlled Space Physics Experiments

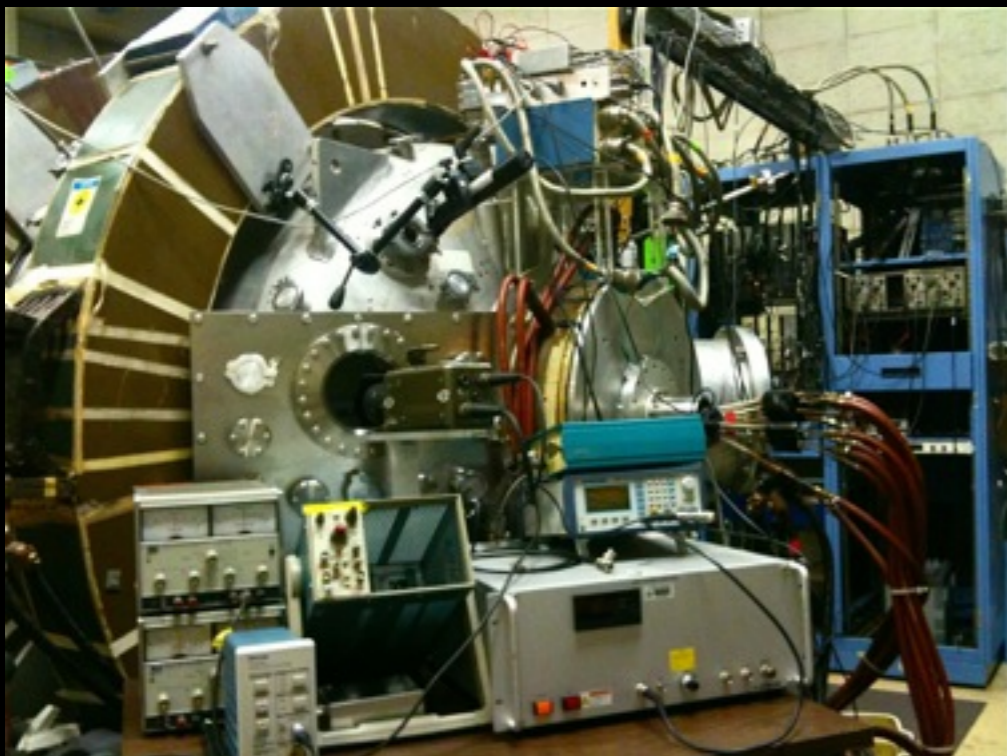


LDX:
High Beta Levitation & Turbulent Pinch



24 Probes
1 m Radius

Ryan



CTX:
Polar Imaging,
Current Injection,
Rotation



Max

Outline

- How does a laboratory magnetosphere work?
- Interchange disturbances and magnetic drift resonances
 - ▶ **Low frequency interchange turbulence: the remarkable “pinch” of magnetized plasma resulting in “canonical” profiles**
 - ▶ **Fast kinetic interchange instabilities: “plasma storms” in the lab**
- **Examples:** exploring plasma dynamics by injection of heat, particles, current, and magnetic perturbations by decreasing ion inertial lengths

LDX and CTX Team

R. Bergmann, A. Boxer, D. Boyle, D. Brennan, M. Davis, G. Driscoll, R. Ellis, J. Ellsworth, S. Egorov, D. Garnier, B. Grierson, O. Grulke, C. Gung, A. Hansen, K.P. Hwang, V. Ivkin, J. Kahn, B. Kardon, I. Karim, J. Kesner, S. Kochan, V. Korsunsky, R. Lations, B. Levitt, S. Mahar, D. Maslovsky, M. Mael, P. Michael, E. Mimoun, J. Minervini, M. Morgan, R. Myatt, G. Naumovich, S. Nogami, E. Ortiz, M. Porkolab, S. Pourrahami, T. Pedersen, A. Radovinsky, A. Roach, M. Roberts, A. Rodin, G. Snitchler, D. Strahan, J. Schmidt, J. Schultz, B. Smith, P. Thomas, P. Wang, H. Warren, B. Wilson, M. Worstell, P. Woskov, B. Youngblood, A. Zhukovsky, S. Zweben



Columbia University



National Science Foundation
WHERE DISCOVERIES BEGIN

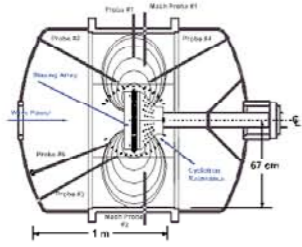




Jay Kesner

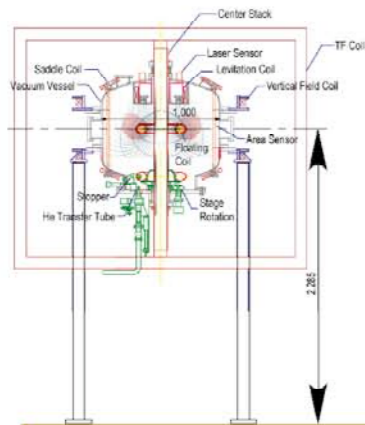
Darren Garnier

Laboratory Dipole Experiments Around the World



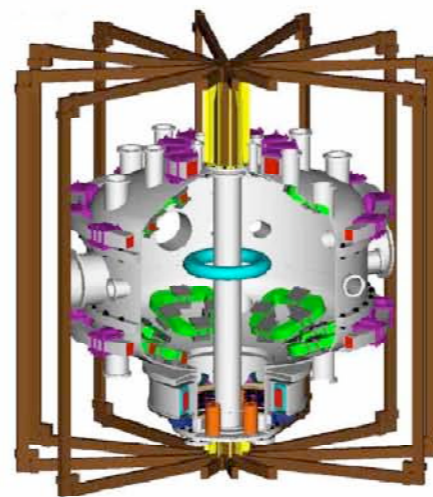
CTX (Columbia)

**150 kA turns
(Not Levitated)
0.15 m**



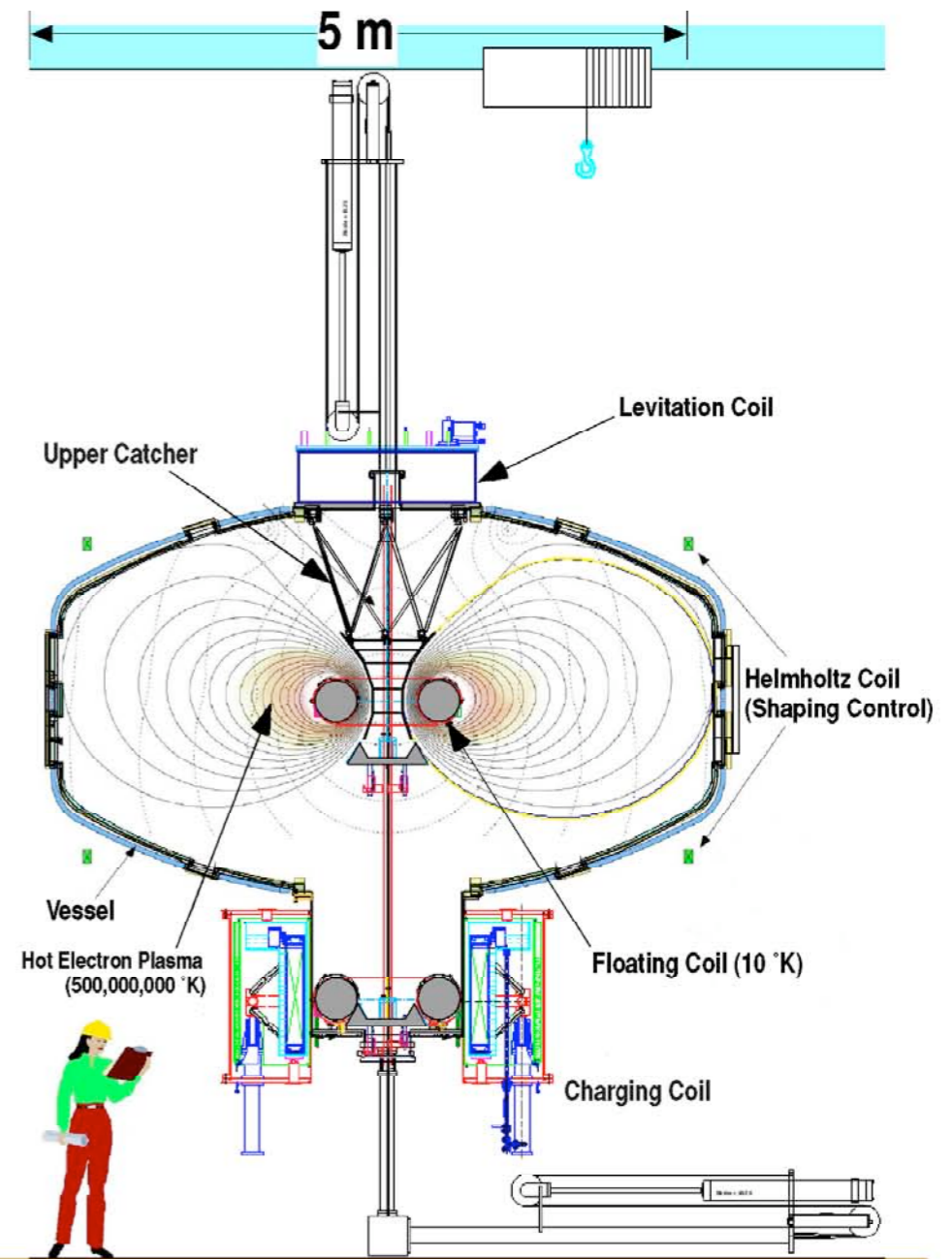
Mini-RT (Univ. Tokyo)

**50 kA turns
17 kg
0.15 m**



RT-1 (Univ. Tokyo)

**250 kA turns
110 kg
0.25 m**



LDX (Columbia-MIT)

**1200 kA turns
565 kg
0.34 m**



Hoist

Levitation Coil

Shaping Coils

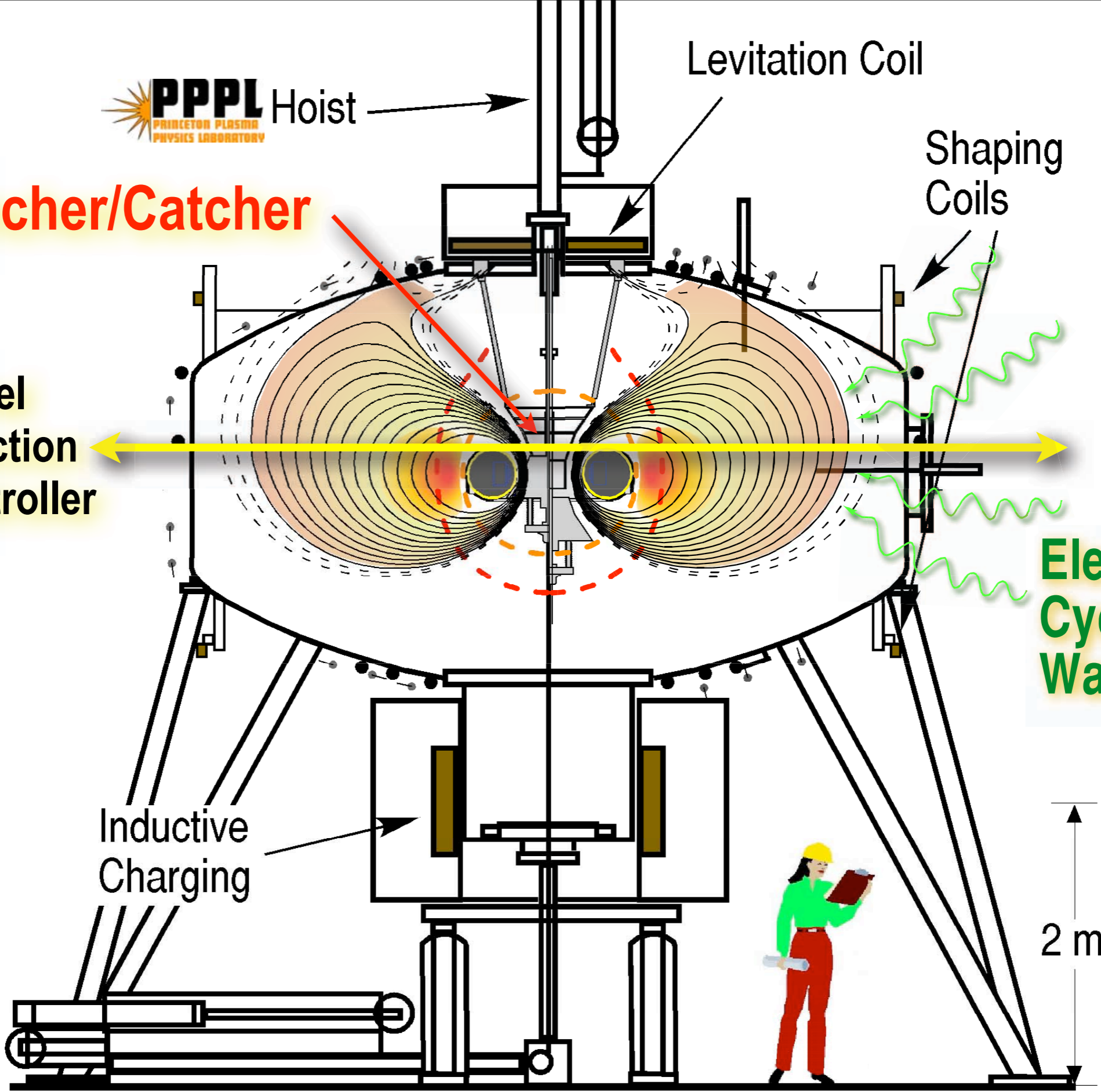
Launcher/Catcher

8 Channel Laser Detection and RT Controller

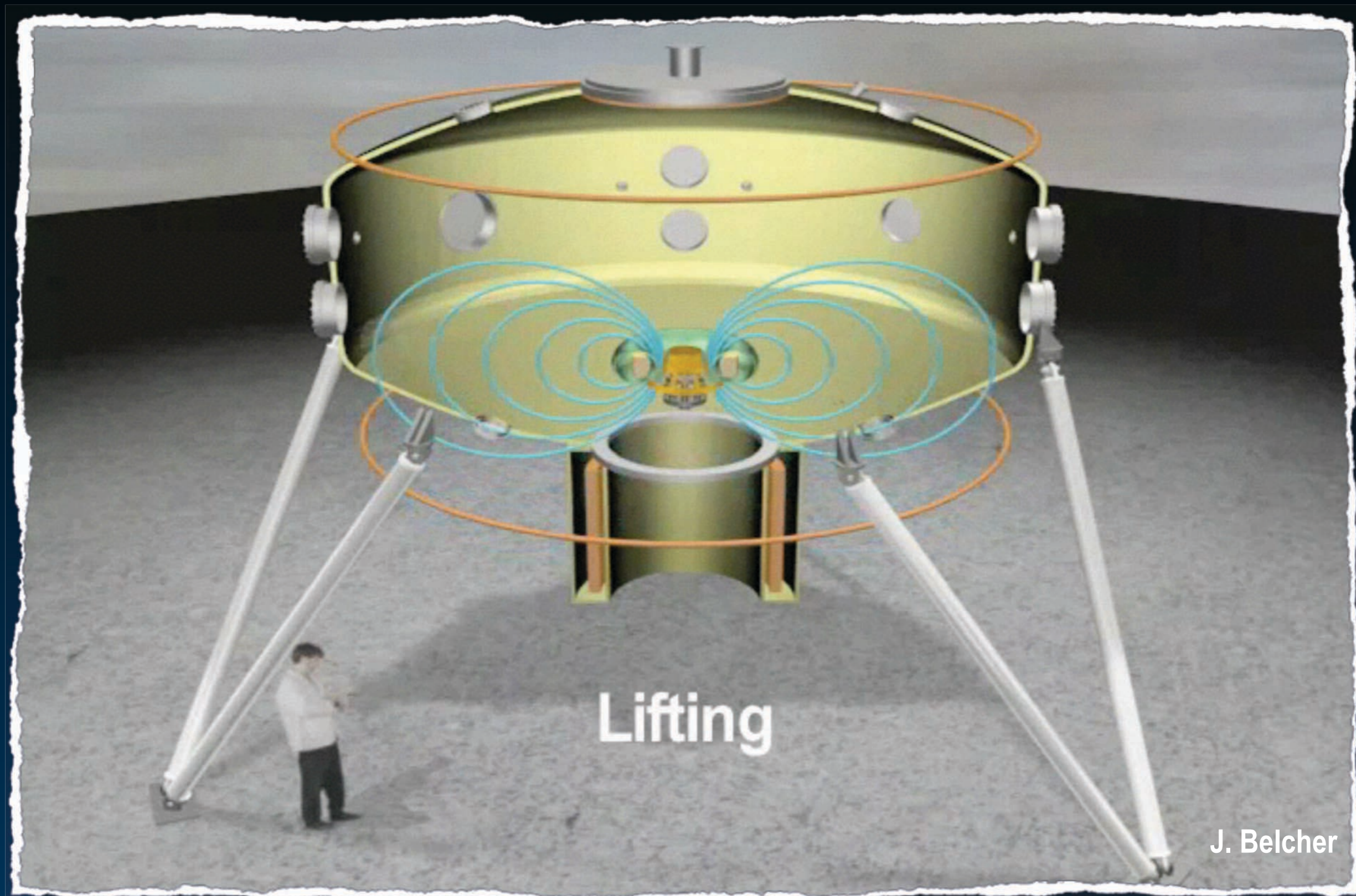
Electron Cyclotron Waves

Inductive Charging

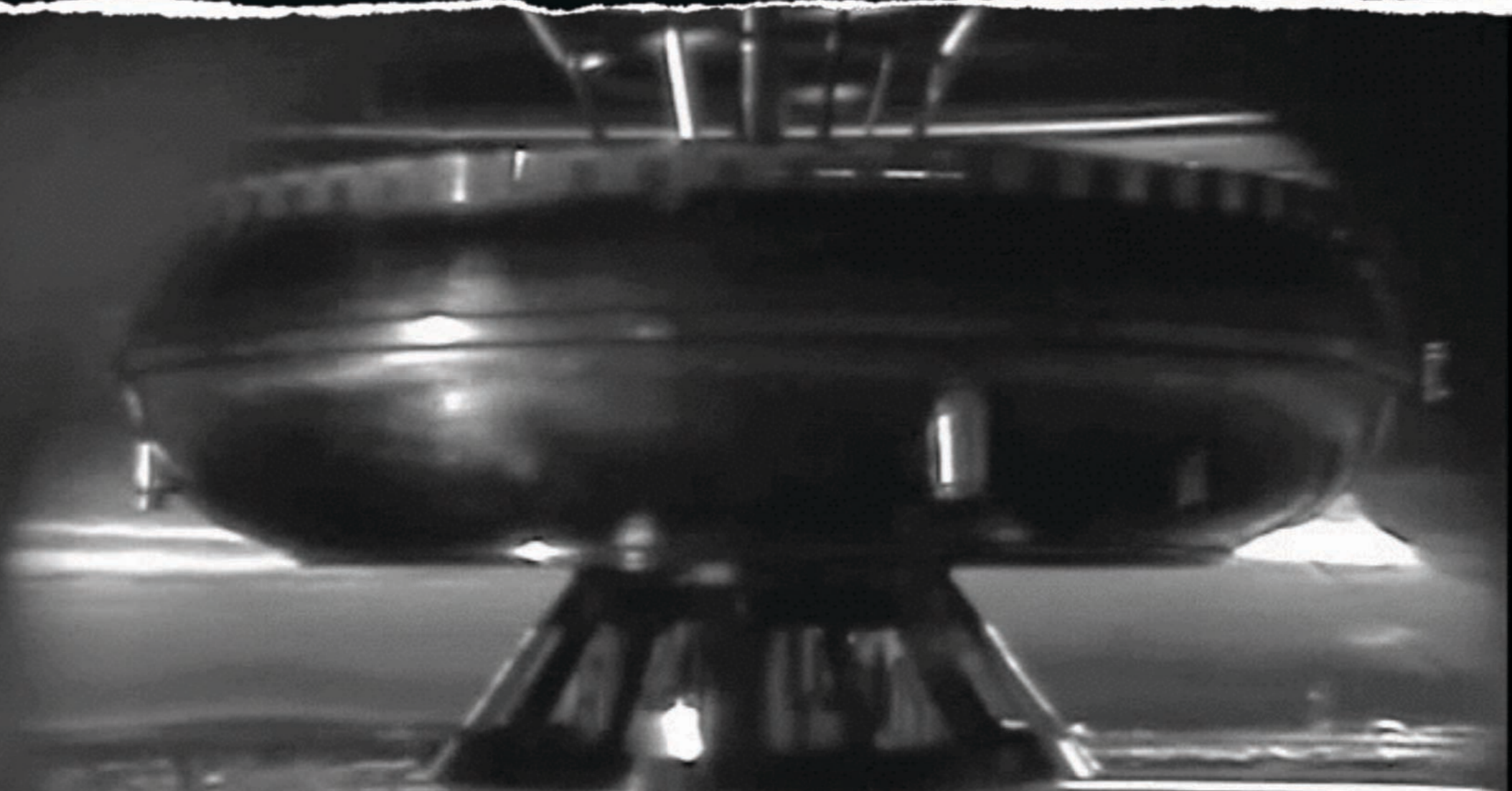
2 m



Lifting, Launching, Levitation, Experiments, Catching

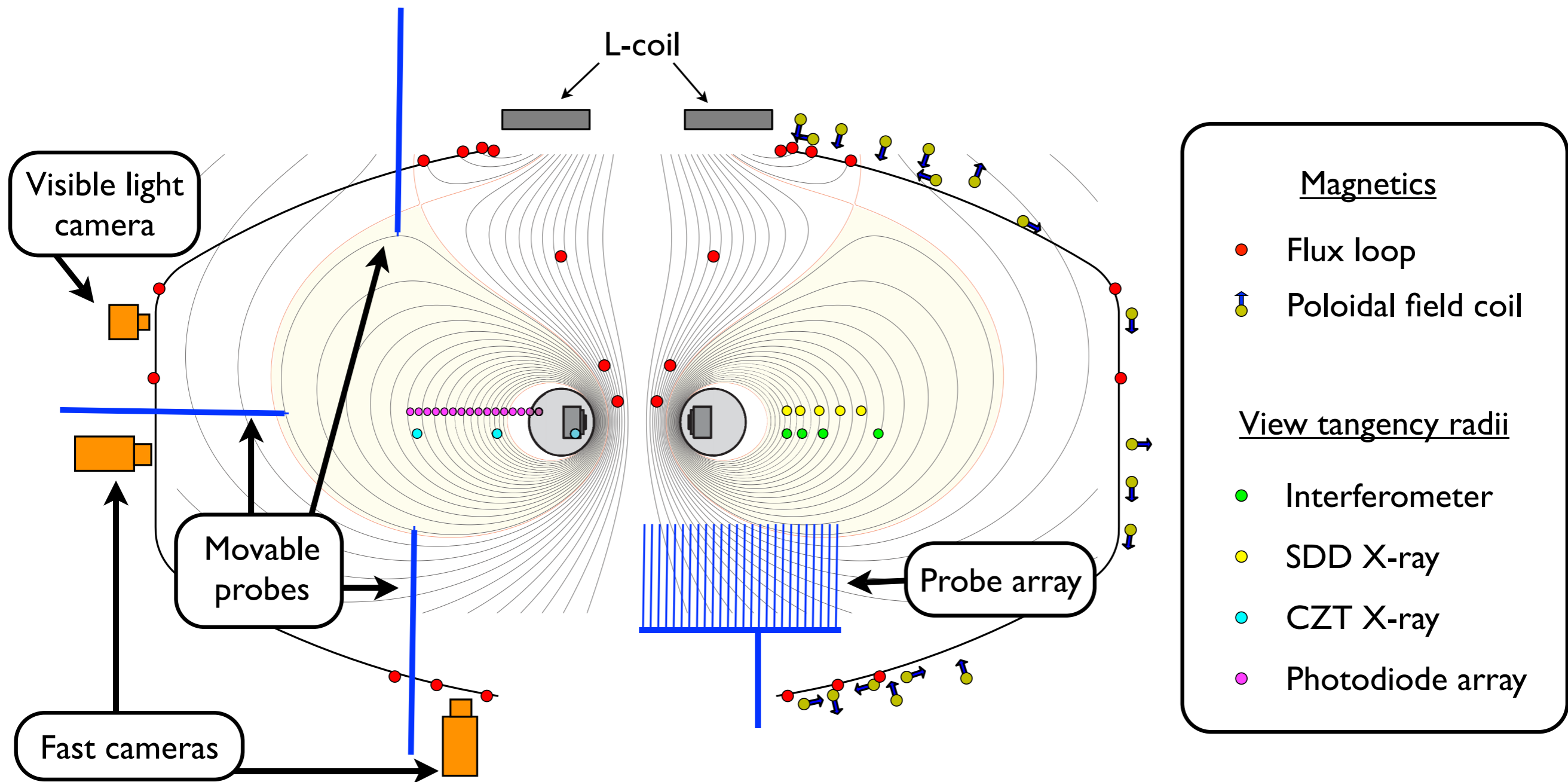


First Levitated Dipole Plasma Experiment



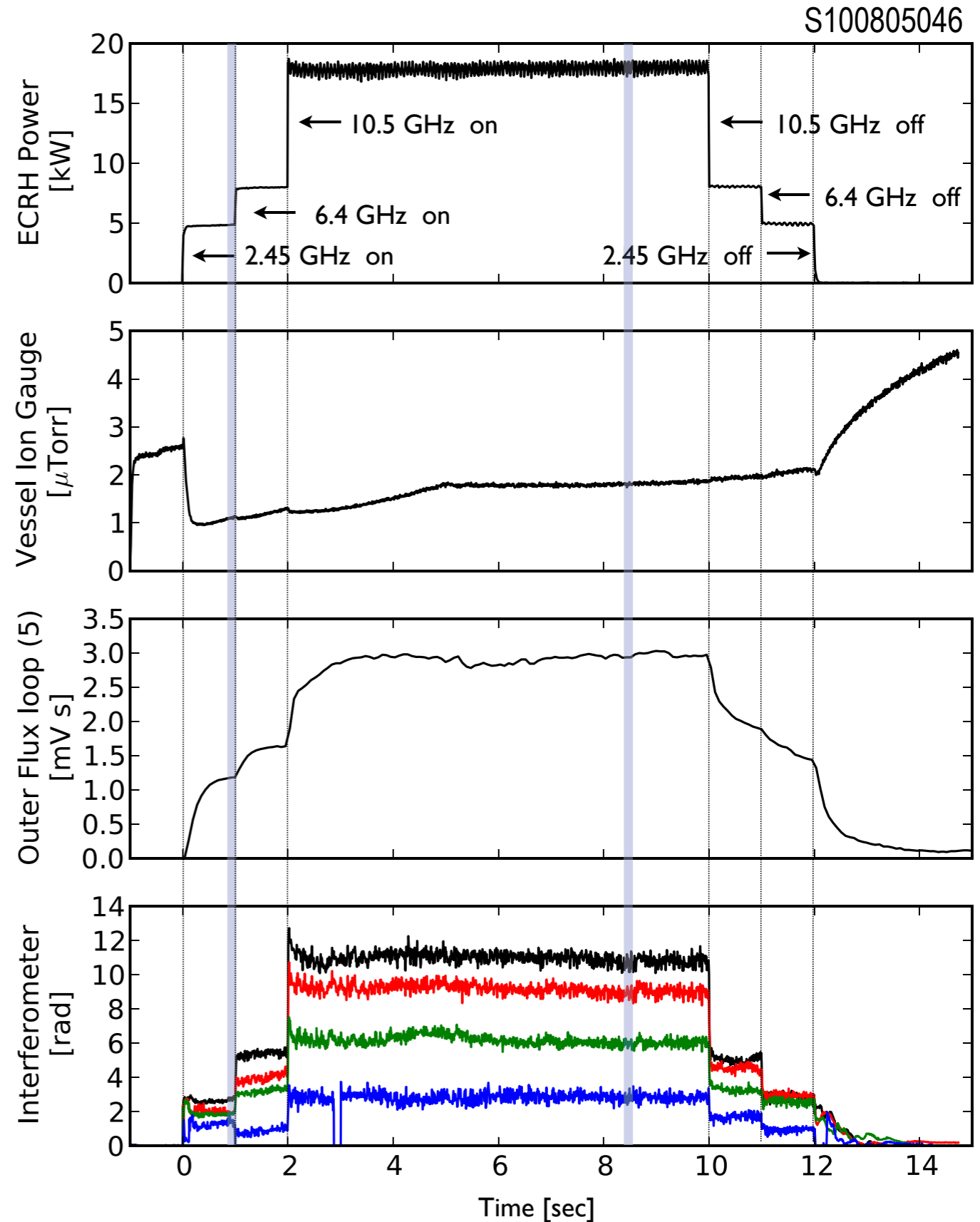
**Floating
(Up to 3 Hours)**

Diagnosics



Example Plasma Experiment

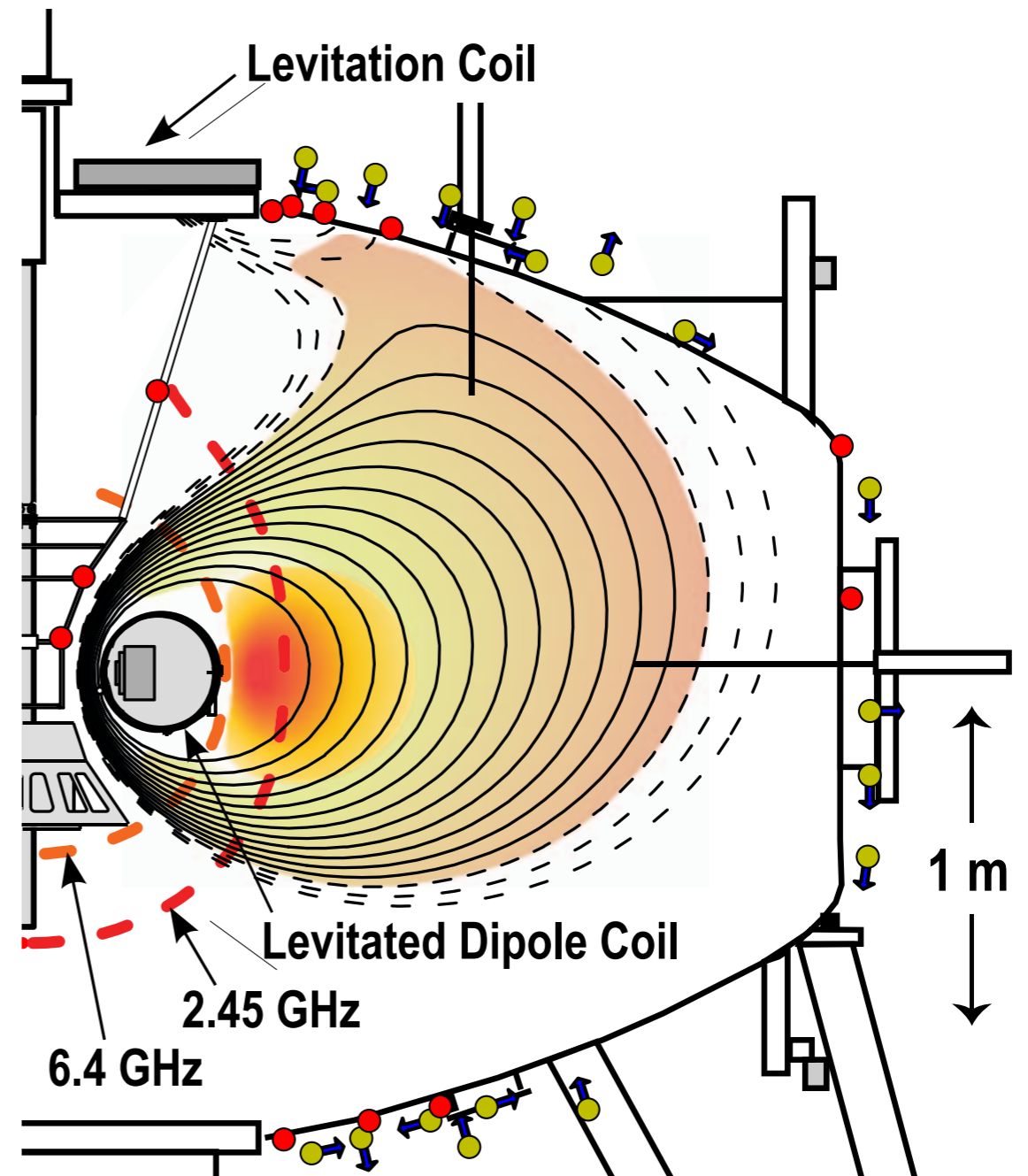
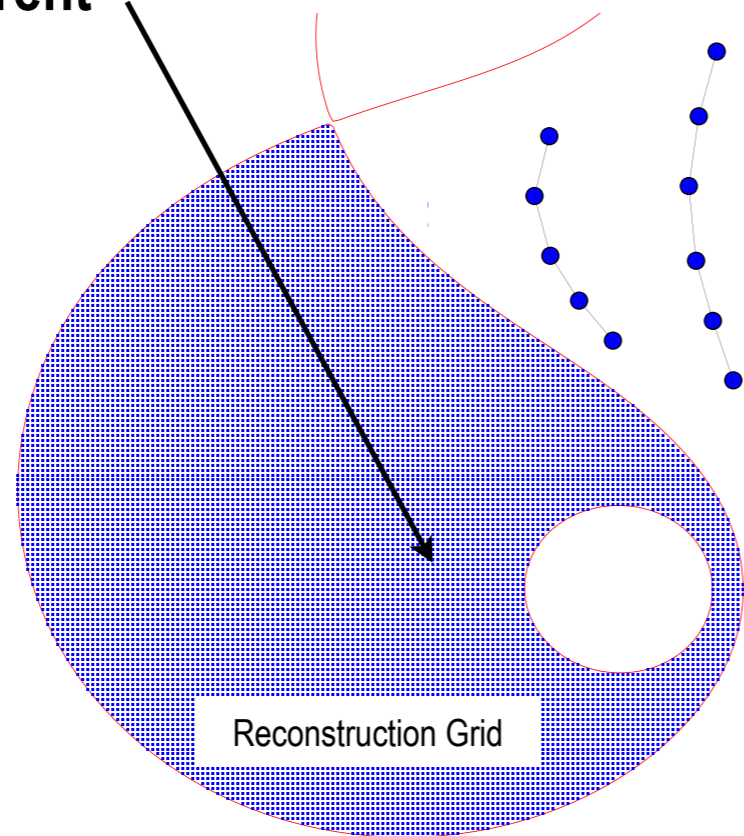
- 20 kW injected electron cyclotron waves
- Hydrogen gas density $4 \times 10^{10} \text{ cm}^{-3}$
- Plasma energy 250 J (3 kA ring current)
- Peak $\beta \sim 40\%$ (70% achieved in RT-1)
- Peak plasma density 10^{12} cm^{-3}
- Peak $\langle T \rangle > 1.4 \text{ keV}$ (electrons)
- Density proportional to injected power
- Sustained, dynamic, “steady state”



Measuring the Plasma Pressure from the Plasma Ring Current

$$\mathbf{J}_{\perp} = \frac{\mathbf{B} \times \nabla P_{\perp}}{B^2} + \frac{\mathbf{B} \times \kappa}{B^2} (P - P_{\perp})$$

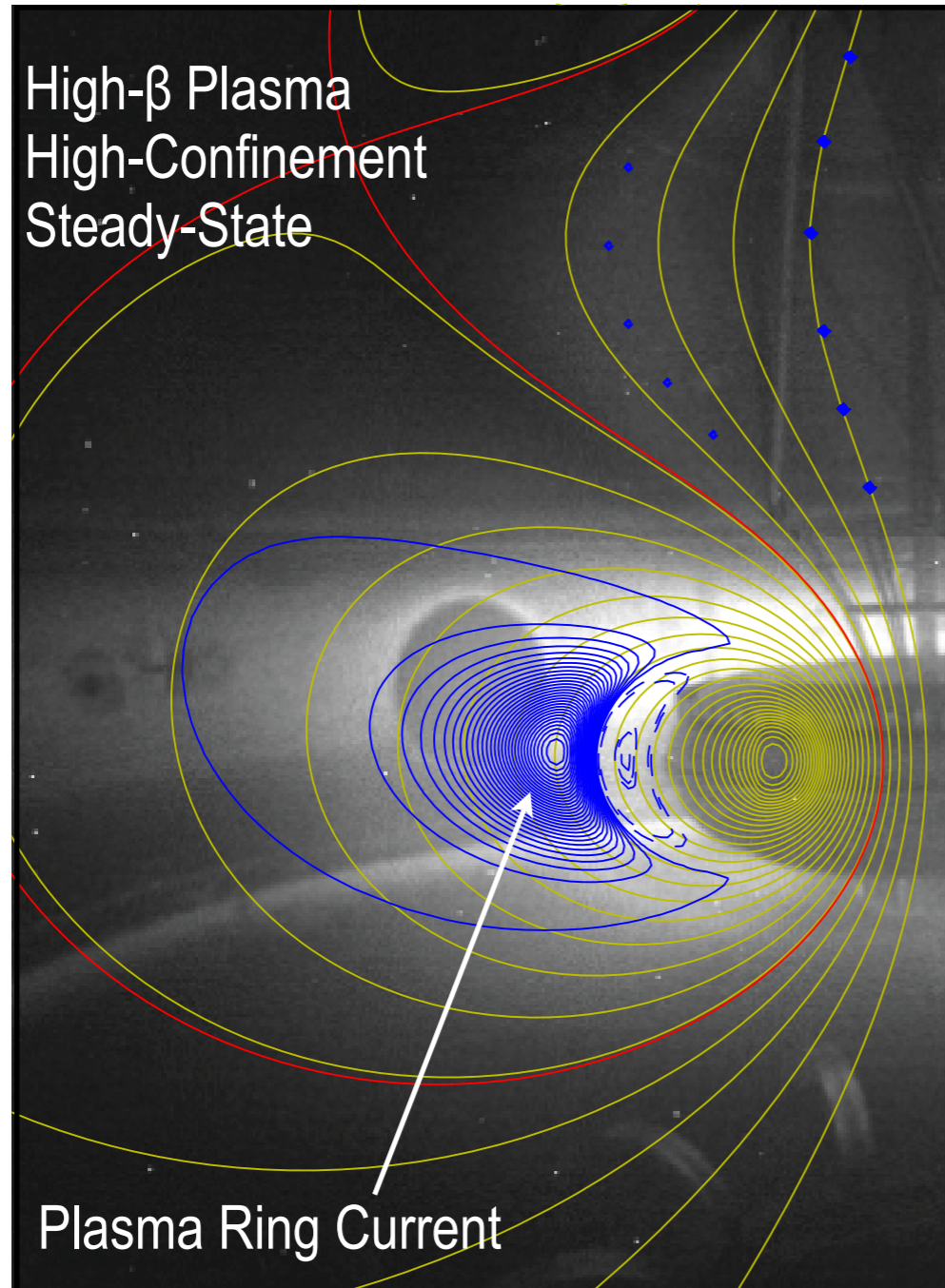
Plasma Ring Current



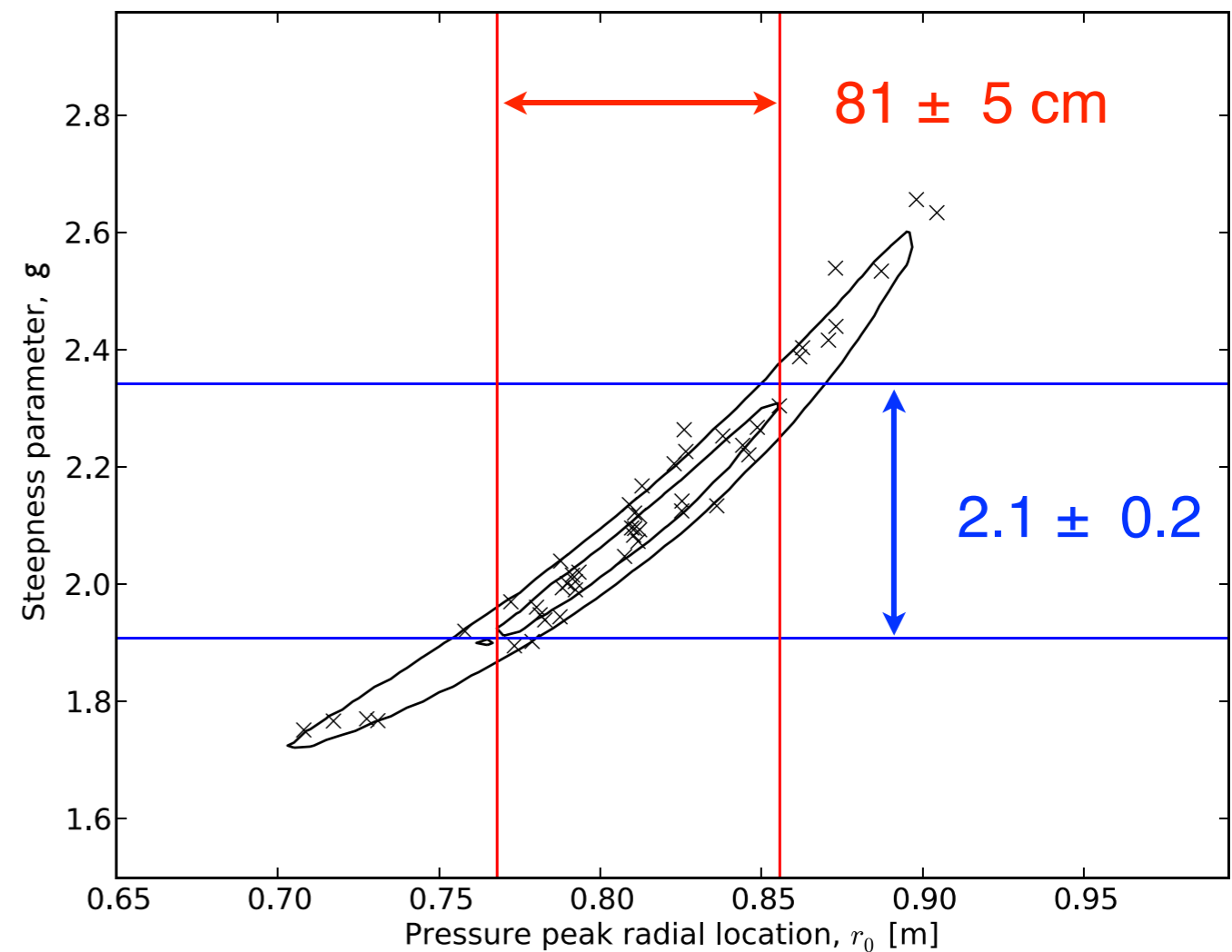
What is the plasma ring current distribution that fits magnetic sensor arrays?

Measuring the Plasma Pressure from the Plasma Ring Current

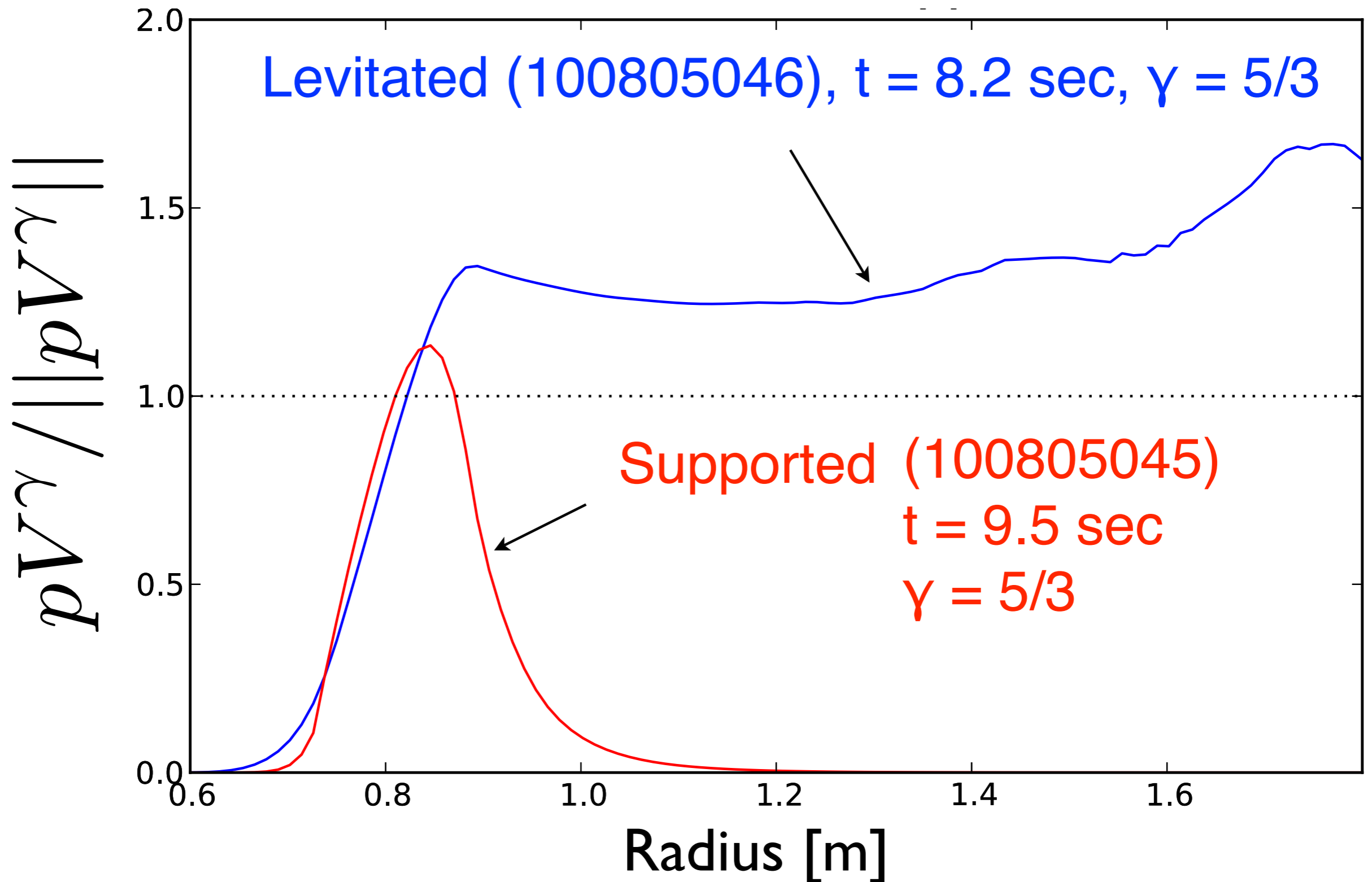
$$\mathbf{J}_{\perp} = \frac{\mathbf{B} \times \nabla P_{\perp}}{B^2} + \frac{\mathbf{B} \times \kappa}{B^2} (P - P_{\perp})$$



Reconstruction Results in Very Good Accuracy of Pressure Profile

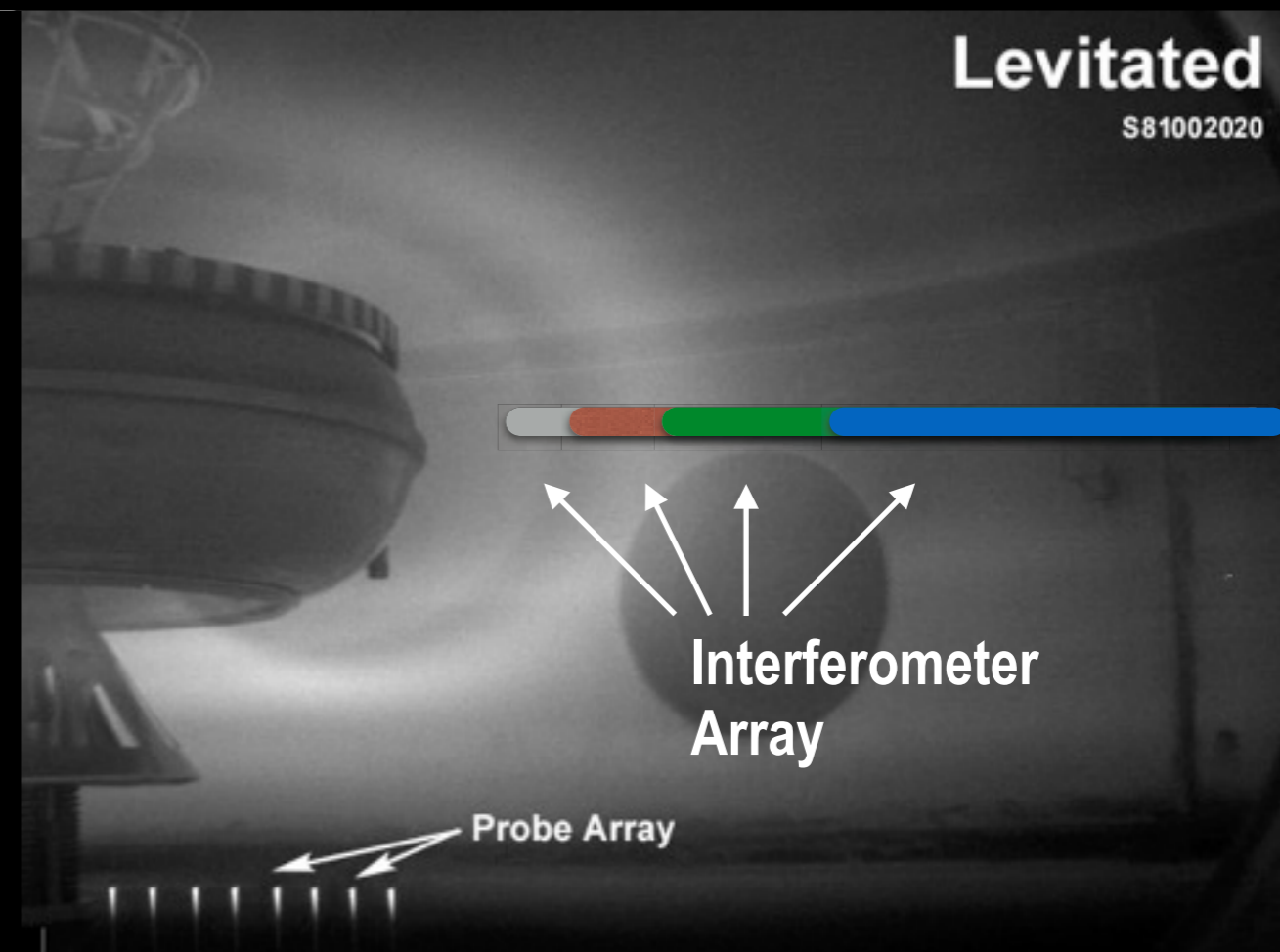
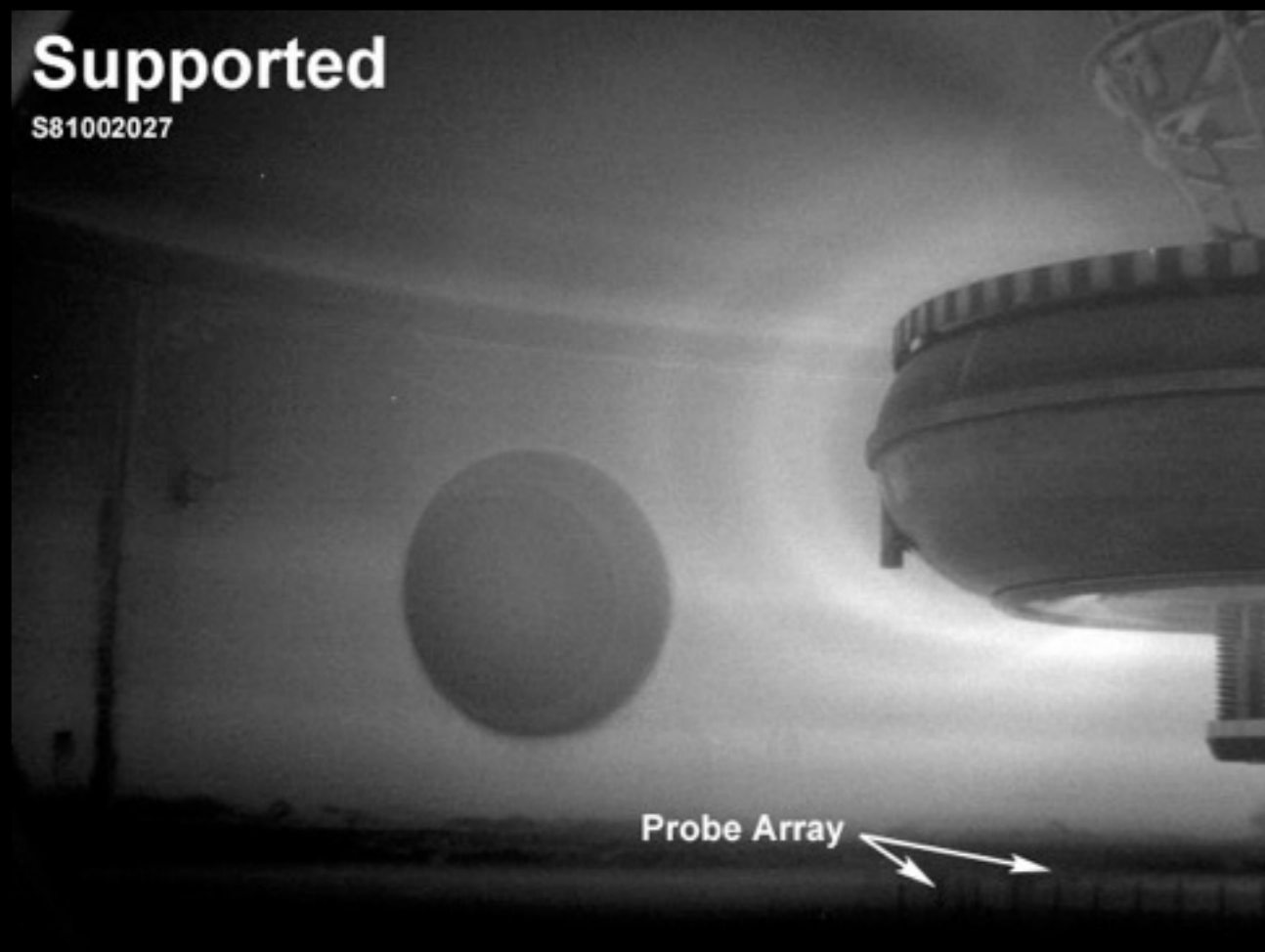


“Canonical” Profile: $\delta(PV^\gamma) \approx 0$



Measurement of Density Profile with Interferometry

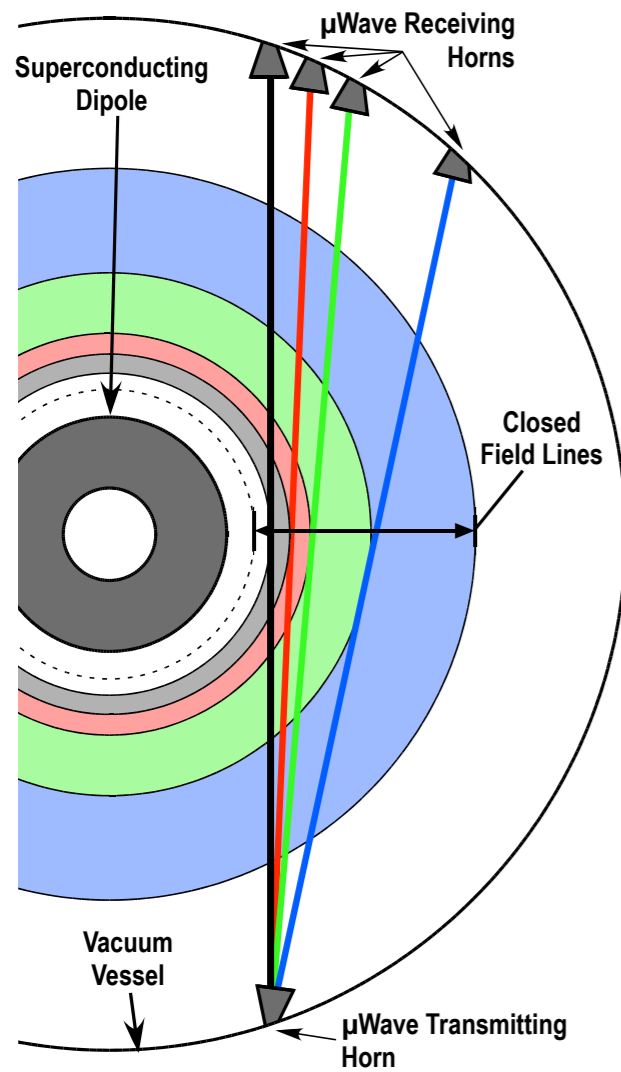
← 5 m →



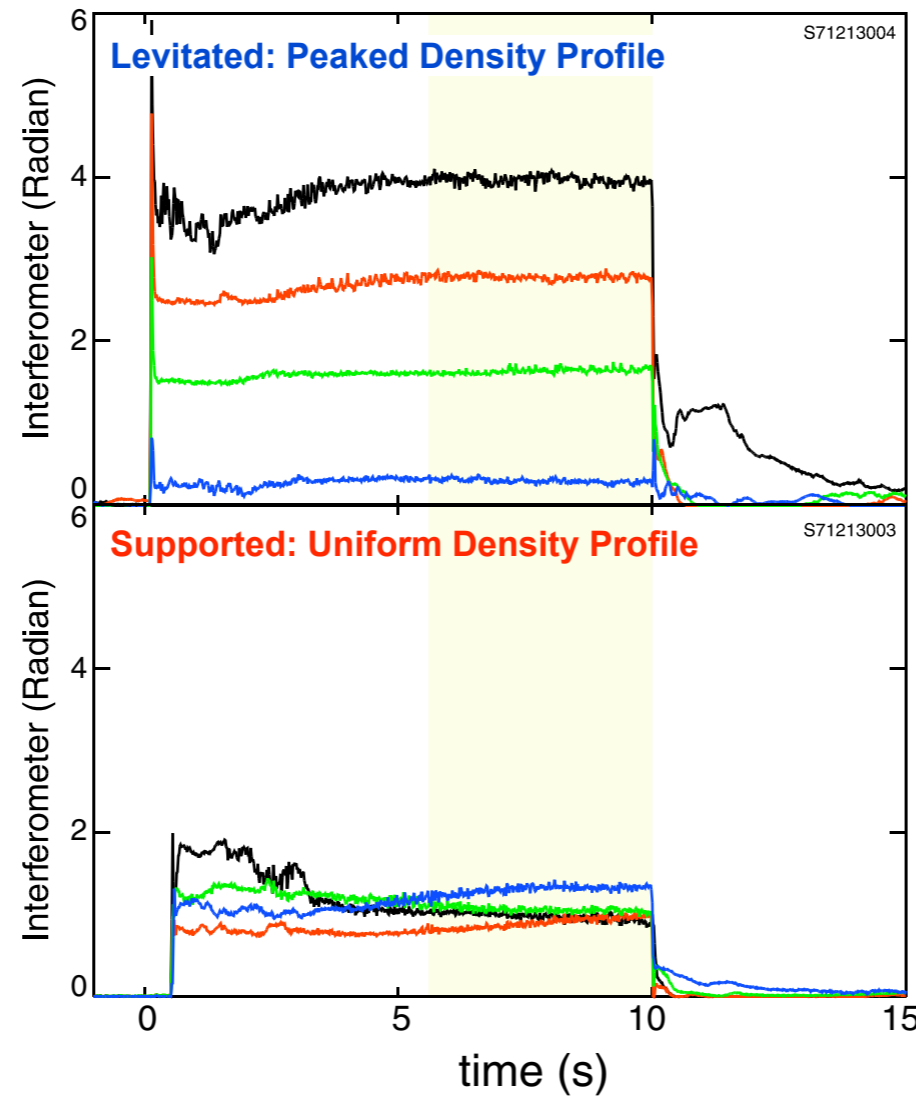
Measurement of Density Profile with Interferometry

Show Equal Particle Number per Unit Magnetic Flux

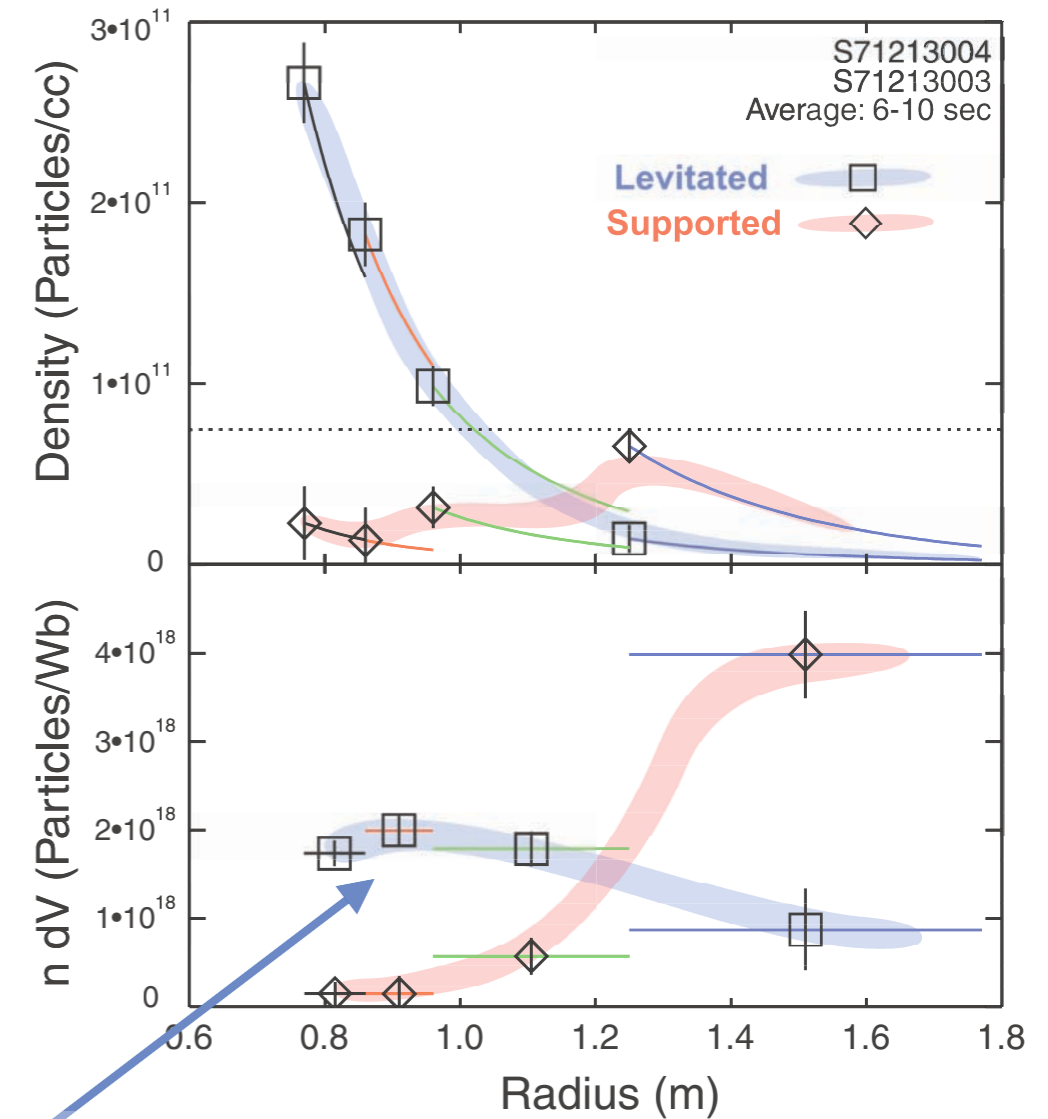
(a) Interferometer Cords



(b) Interferometer Measurements



(c) Density and Number Radial Profiles



“Canonical” Profile: $\delta(nV) \approx 0$

Remarkable “Pinch”: Dye Stirred in Glass



“Canonical” Profiles of Magnetized Plasma

$$\delta(nV) \approx 0 \quad \& \quad \delta(PV^\gamma) \approx 0$$

- Low frequency fluctuations in strongly magnetized plasma, $\omega \ll \omega_b \ll \omega_c$, conserve constants of motion.
- **Turbulent mixing across flux tube volumes tries to “relax” to the canonical profiles**, which are Lagrangian invariants of the flow. Turbulence in strongly magnetized plasma tries to **“self organize”**.
- **Magnetic flux-tube geometry** relates turbulent diffusion in magnetic-flux-space to diffusive and pinch terms in coordinate-space.
- **Space (i.e. Dipole) geometry:**
 - ➔ Birmingham, *J. Geophysical Res.*, 1969
 - ▶ Kobayashi, Rogers, and Dorland, *Phys. Rev. Lett.*, 2010
 - ▶ Kesner, *et al.*, *Plasma Phys. Control. Fusion*, 2010; Kesner, *et al.*, *Phys. Plasmas*, 2011.
- **Tokamak geometry:**
 - ➔ Coppi, *Comments Plasma Phys. Controll. Fus.*, 1980
 - ▶ Yankov, *JETP Lett.*, 1994 and Isichenko, *et al.*, *Phys. Rev. Lett.*, 1995
 - ▶ Baker and Rosenbluth, *Phys. Plasmas*, 1998; Baker, *Phys. Plasmas*, 2002
 - ▶ Garbet, *et al.*, *Phys. Plasmas*, 2005

Convection Electric Fields and the Diffusion of Trapped Magnetospheric Radiation

THOMAS J. BIRMINGHAM

$$\mathbf{E} \times \mathbf{B} \quad \left\{ \dot{\psi} = \nabla \psi \cdot \mathbf{V} = \frac{\partial \Phi}{\partial \varphi} = -RE_{\varphi} \right.$$

$$\text{Diffusion Coefficient} \quad \left\{ \begin{aligned} D_{\psi} &= \lim_{t \rightarrow \infty} \int_0^t dt \langle \dot{\psi}(t) \dot{\psi}(0) \rangle \equiv \langle \dot{\psi}^2 \rangle \tau_c \\ &= R^2 \langle E_{\varphi}^2 \rangle \tau_c \end{aligned} \right.$$

$$\text{Adiabatic Radial Transport} \quad \left\{ \frac{\partial F}{\partial t} = S + \frac{\partial}{\partial \psi} \Big|_{\mu, J} D_{\psi}(\mu, J) \frac{\partial F}{\partial \psi} \Big|_{\mu, J} \right.$$

NORAD OV3-4 (1966) validated physics of inward pinch and adiabatic heating of drift-resonant radiation belt particles. Farley, *et al.*, *Phys. Rev. Lett.*, 1970

Turbulent Pinch in Toroidal Laboratory Plasmas

When the turbulent spectrum is sufficiently broad to interact with (nearly) all particles, *independent of energy and pitch-angle*, then ...

Flux-Tube **Particle** Number Transport:

$$\begin{aligned} \frac{\partial(\bar{n}\delta V)}{\partial t} &= \langle S \rangle + \frac{\partial}{\partial\psi} D_\psi \frac{\partial(\bar{n}\delta V)}{\partial\psi} \\ &= \langle S \rangle + \frac{\partial}{\partial\psi} \left[\underbrace{D_\psi \delta V}_{\text{Diffusion}} \frac{\partial\bar{n}}{\partial\psi} + \bar{n} \underbrace{D_\psi \frac{\partial\delta V}{\partial\psi}}_{\text{Pinch Velocity}} \right] \end{aligned}$$

Flux-Tube Plasma **Energy/Entropy** Transport:

$$\frac{\partial(\bar{P}\delta V^\gamma)}{\partial t} = \langle H \rangle + \frac{\partial}{\partial\psi} D_\psi \frac{\partial(\bar{P}\delta V^\gamma)}{\partial\psi}$$

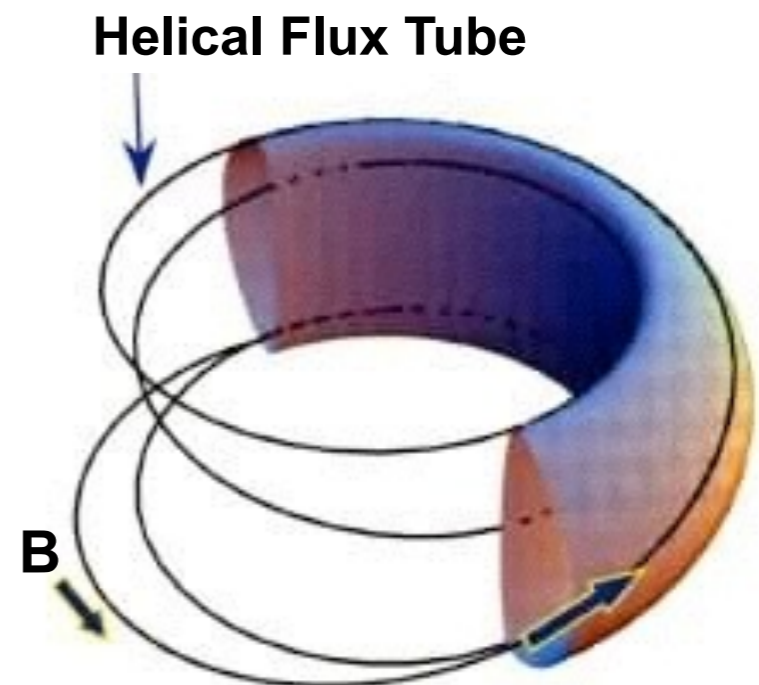
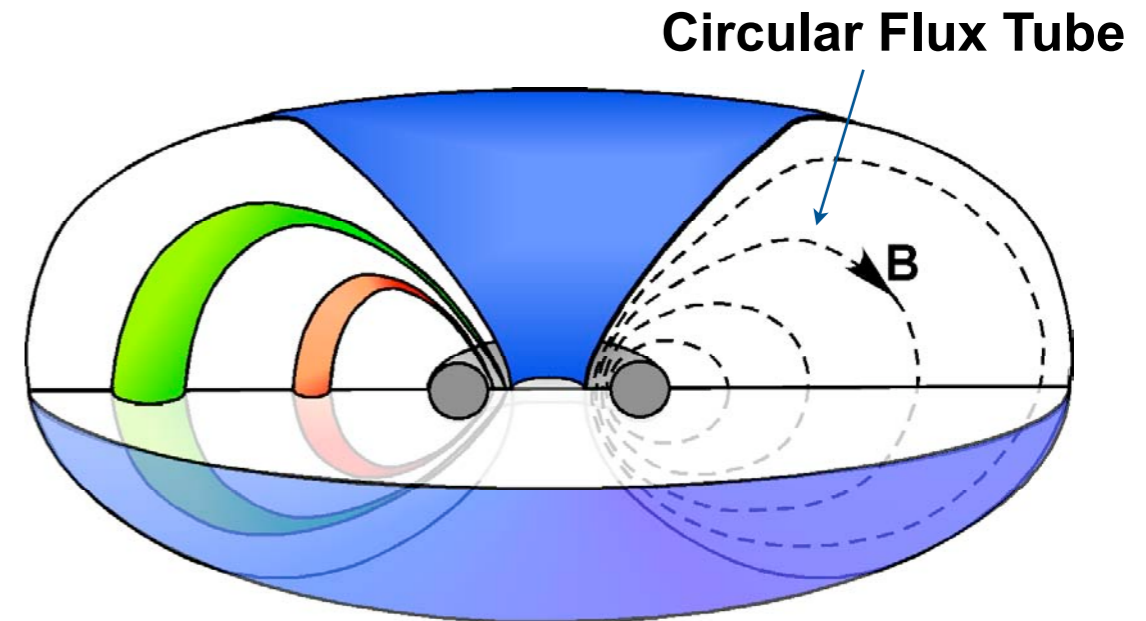
Magnetic flux-tube geometry sets low frequency dynamics

● Dipole...

- ▶ Interchange sets pressure and density gradient limits in dipole-plasma (*compressibility not average good curvature*) with $\beta \sim 100\%$
- ▶ Flux-tubes can interchange globally without bending (*no magnetic shear*)
- ▶ No toroidally circulating particles: all particles have similar response to low-frequencies
- ➔ **Flux tube volume increases rapidly** with radius, $V \sim 1/L^4$, resulting in steep profiles

● Tokamak...

- ▶ Ballooning and kinks set pressure limit with $\beta \sim \epsilon/q \approx 5\%$
- ▶ Short radial scale of fluctuations, drift waves
- ▶ Passing and trapped particle dynamics differ
- ➔ **Flux tube volume nearly constant** with radius, $V \sim 1/q$, mixing creates flat profiles



Geometry of Magnetic Flux Tubes, δV , Determines Pinch

Dipole

$$D_\psi = R^2 \langle E_\varphi^2 \rangle \tau_c$$

Tokamak (Trapped Particles)

$$D_\psi = R^2 \langle E_\theta^2 \rangle (B_p^2 / B^2) \tau_c$$

Flux-Tube Number Transport:

$$\frac{\partial(\bar{n}\delta V)}{\partial t} = \langle S \rangle + \frac{\partial}{\partial \psi} D_\psi \frac{\partial(\bar{n}\delta V)}{\partial \psi} = 0$$

Steady-state *without* internal source, zero net flux condition:

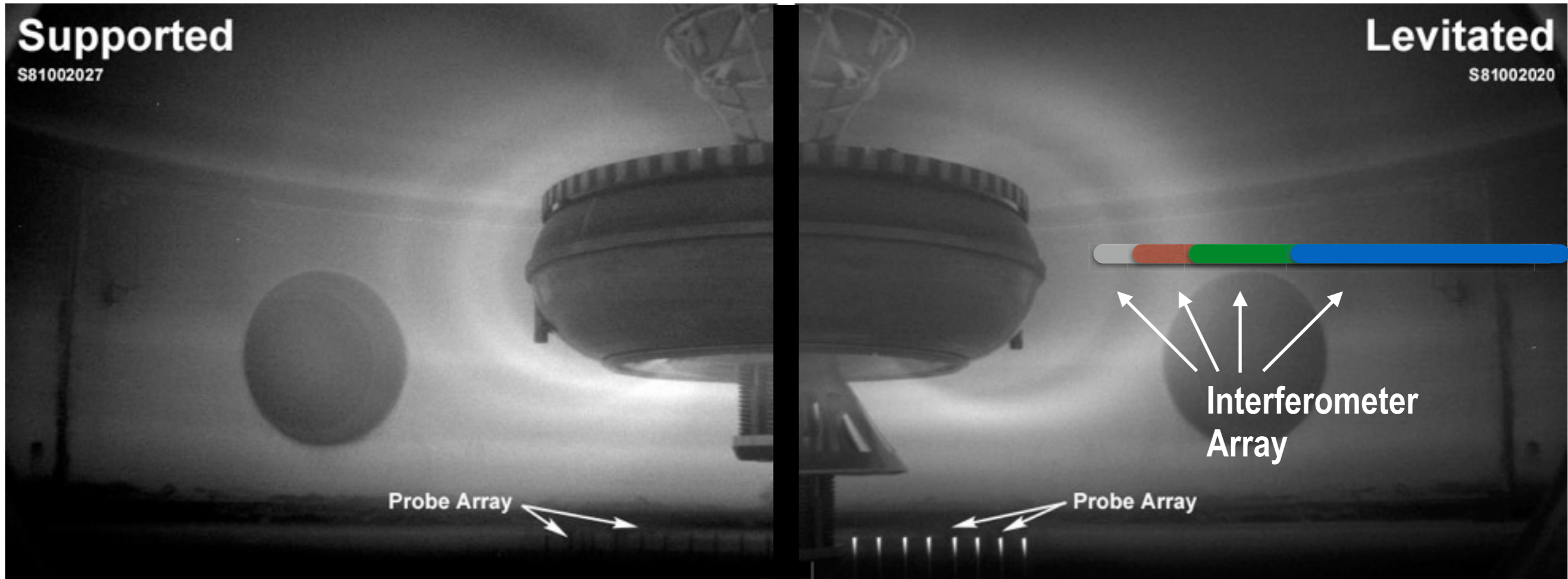
$$\bar{n} \propto \frac{1}{\delta V} \sim \begin{cases} 1/R^4 & \text{Dipole} \\ 1/q & \text{Tokamak (Trapped Particles)} \end{cases}$$

... and particles can move **inward against a density gradient**.

Quantitative Verification of Turbulent Particle Pinch

Using only *measured electric field* fluctuations,
Thomas Birmingham's diffusion model is verified with levitated dipole

5 m

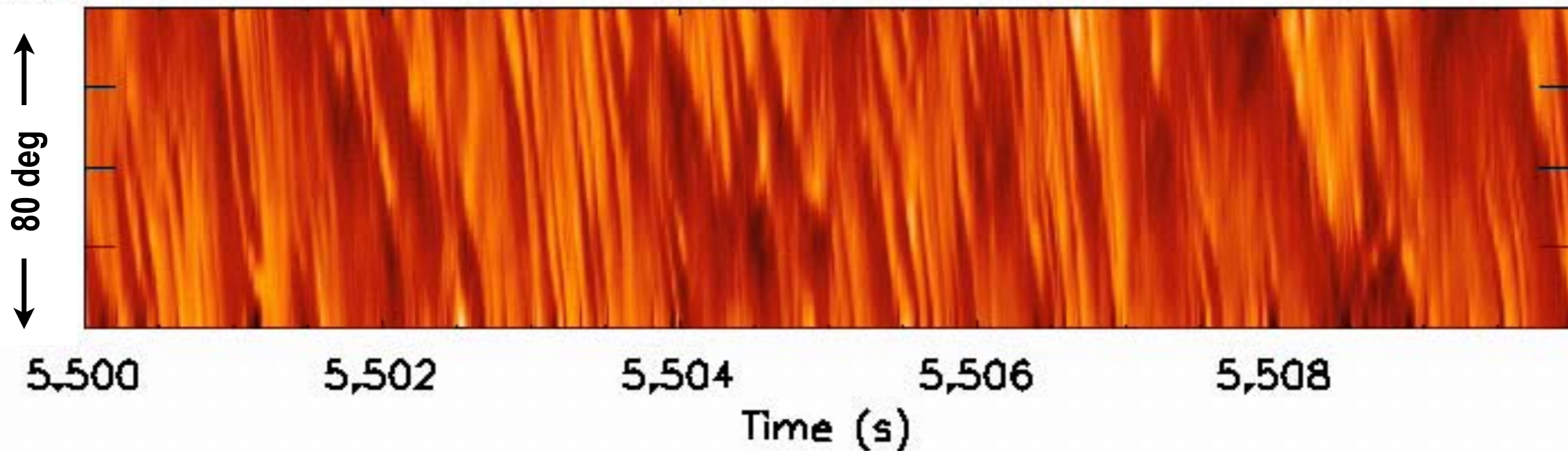


Edge Probe Array:
$$D = \lim_{t \rightarrow \infty} \int_0^t dt \langle \dot{\psi}(t) \dot{\psi}(0) \rangle \equiv \langle \dot{\psi}^2 \rangle \tau_c$$
$$D_\psi = R^2 \langle E_\varphi^2 \rangle \tau_c$$

Quantitative Verification of Turbulent Particle Pinch

Using only *measured electric field* fluctuations,
Thomas Birmingham's diffusion model is verified with levitated dipole

Floating Potential ($\Phi > \pm 150$ V)

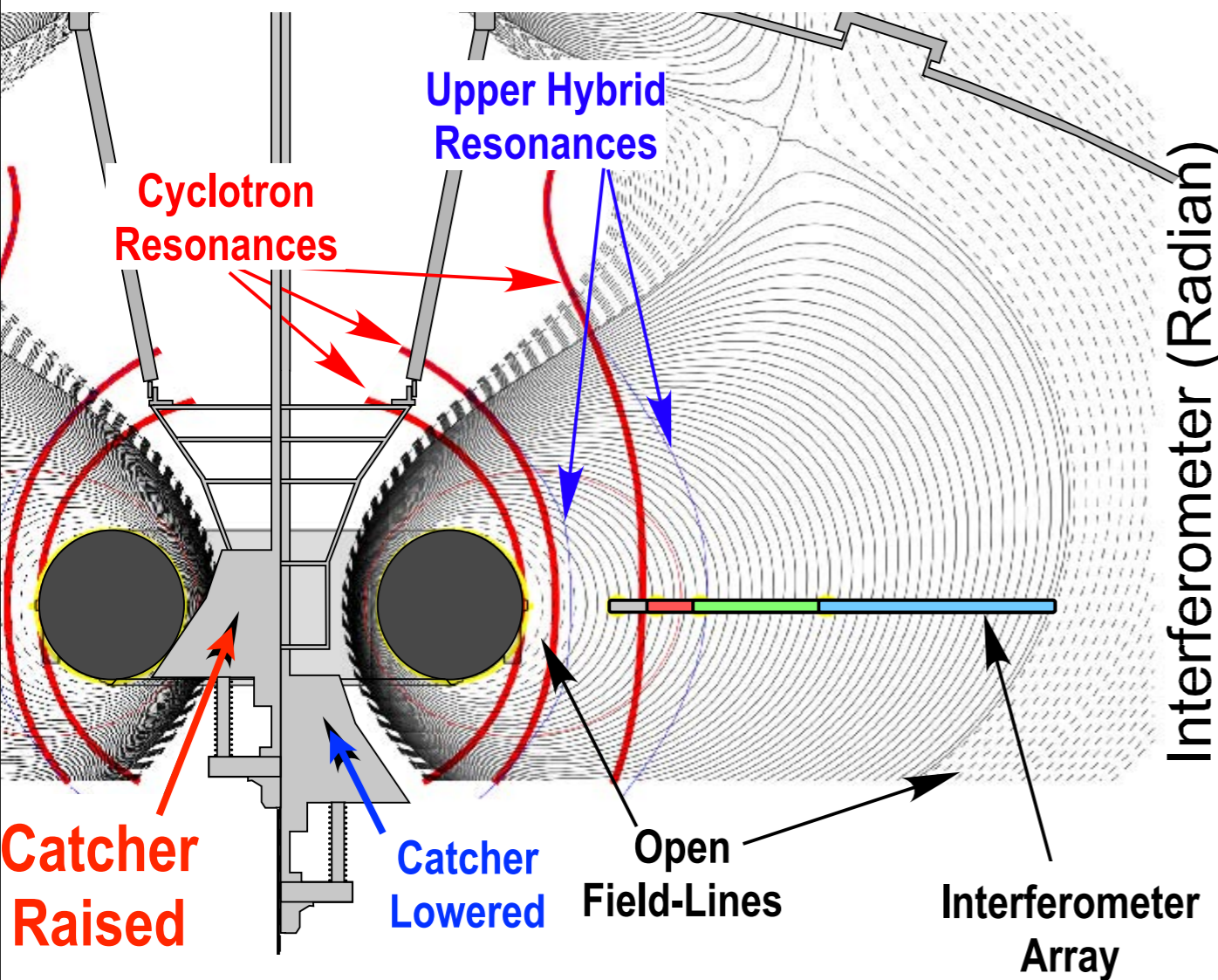


Edge Probe Array:
$$D = \lim_{t \rightarrow \infty} \int_0^t dt \langle \dot{\psi}(t) \dot{\psi}(0) \rangle \equiv \langle \dot{\psi}^2 \rangle \tau_c$$
$$D_\psi = R^2 \langle E_\varphi^2 \rangle \tau_c$$

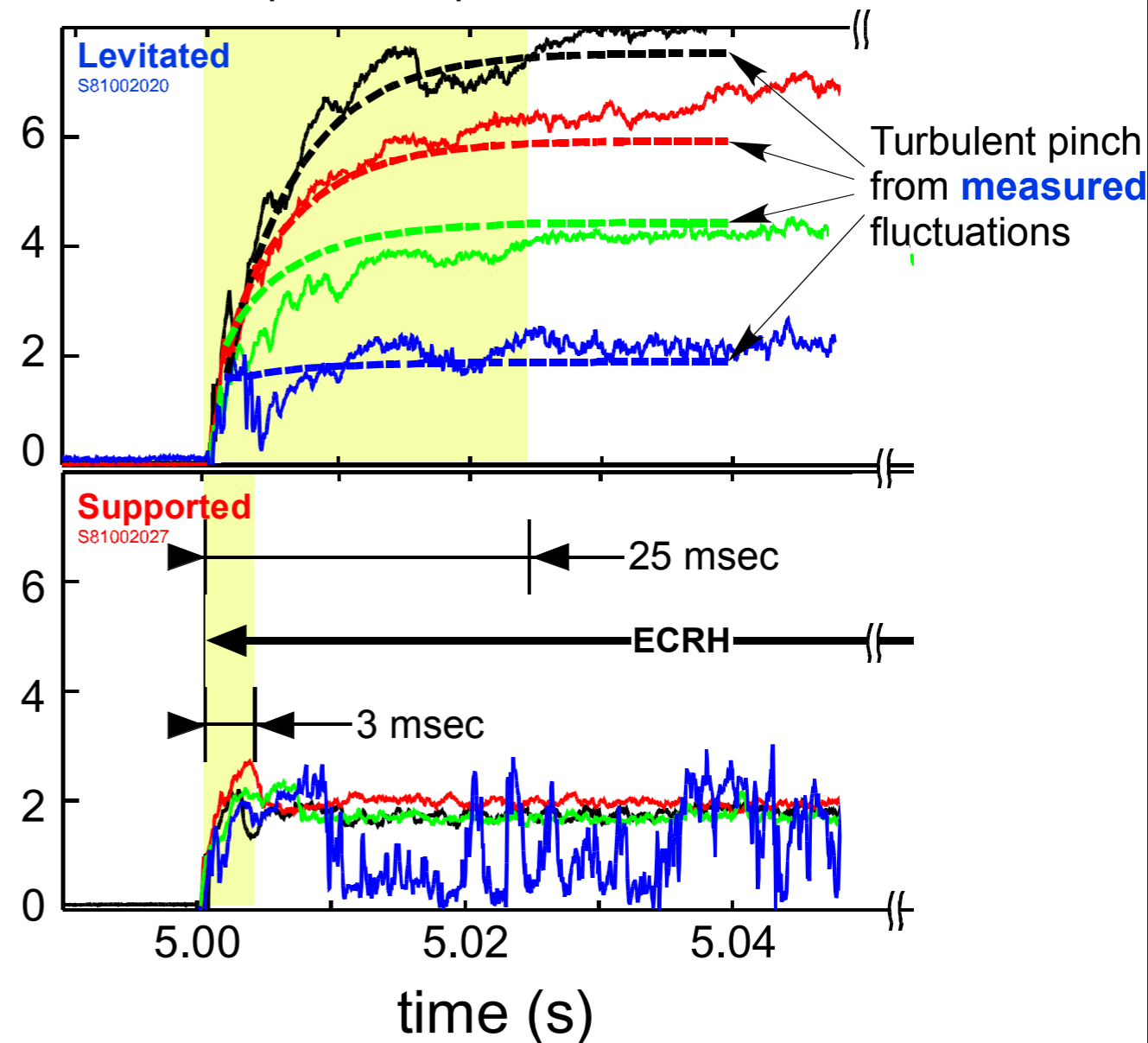
Quantitative Verification of Inward Turbulent Pinch

$$\frac{\partial(\bar{n}\delta V)}{\partial t} = \langle S \rangle + \frac{\partial}{\partial \psi} D_{\psi} \frac{\partial(\bar{n}\delta V)}{\partial \psi}$$

With levitated dipole, inward turbulent transport sets profile evolution

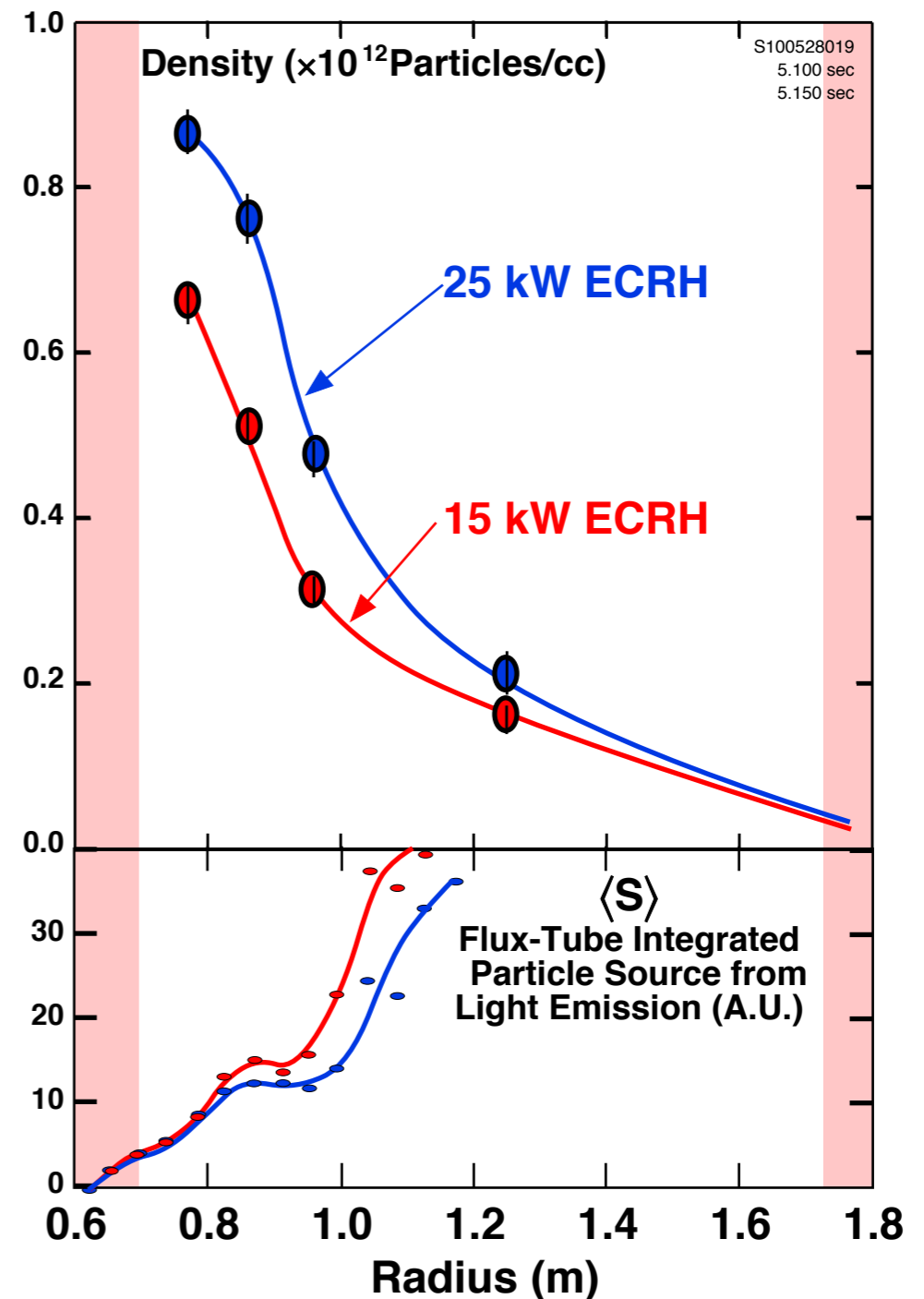
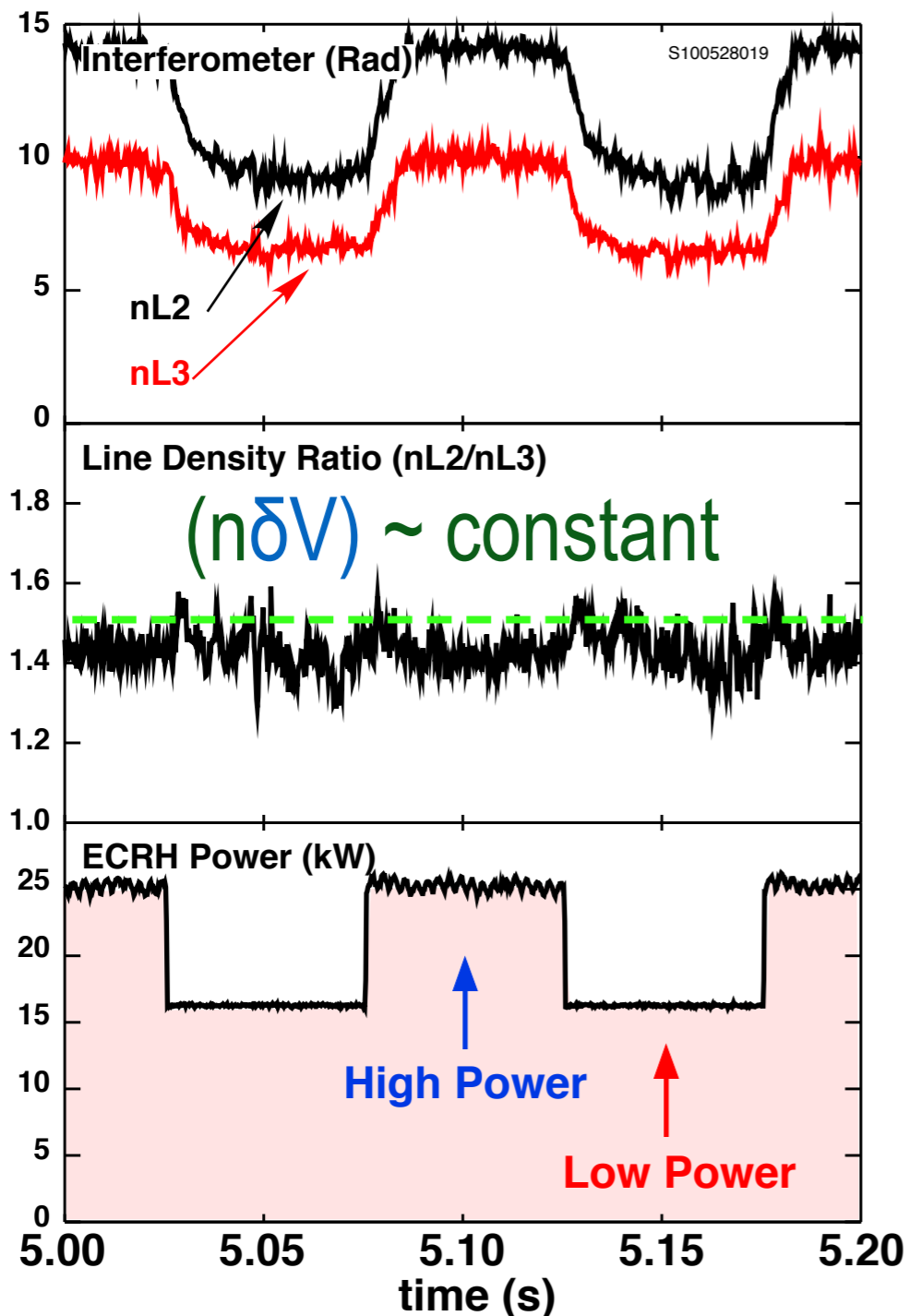


Interferometer (Radian)



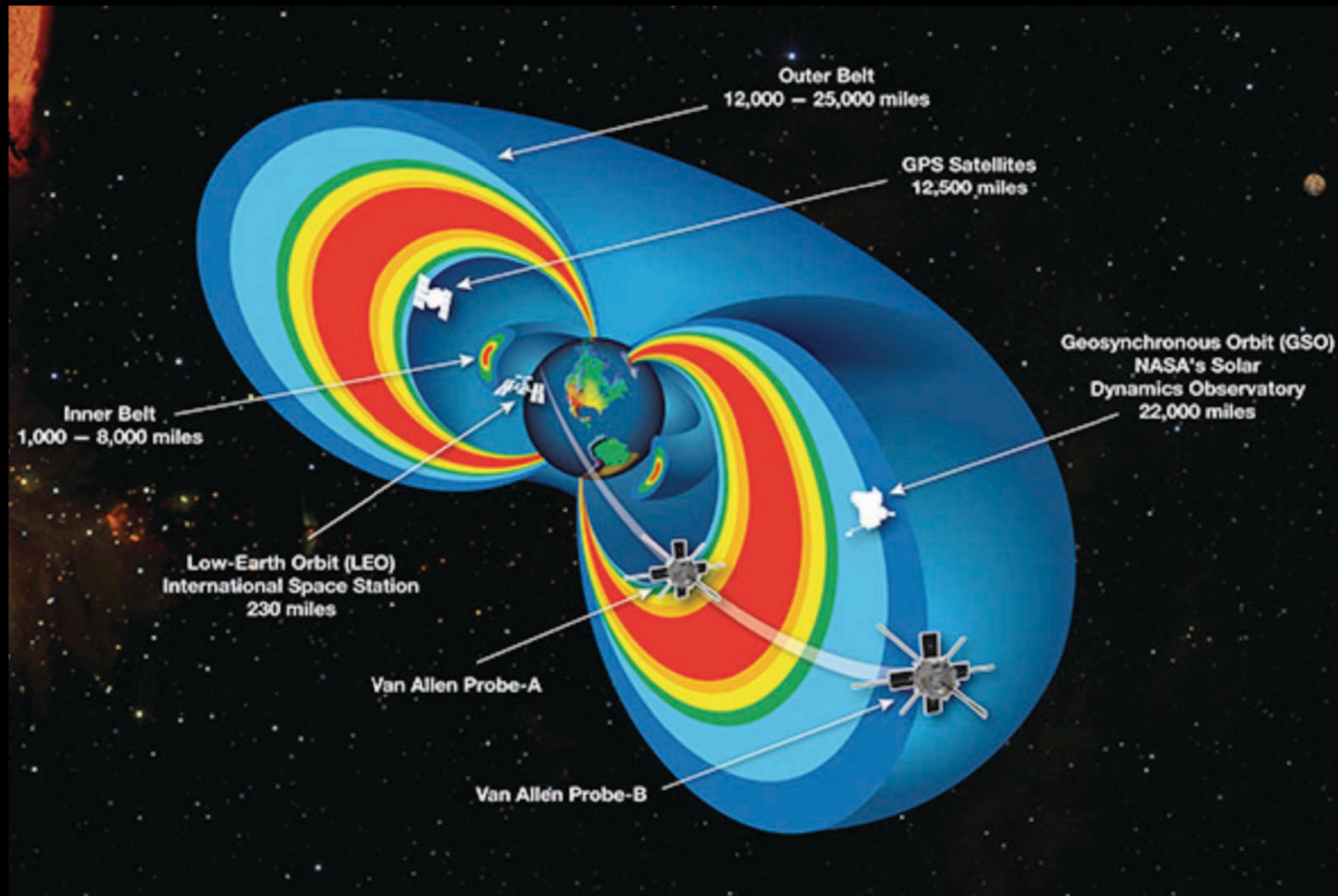
Heating modulation demonstrates robust inward pinch towards invariant profile

- Density increases with power ($T \sim \text{constant}$). Density profile shape is unchanged near $(n\delta V) \sim \text{constant}$.
- Gas source moves radially outward. Inward pinch required to increase central density.



Our Space Environment is Complex and Highly Variable

With Concurrent Plasma Processes and Important Questions to Answer



Van Allen Probes (A&B) Launched August 2012

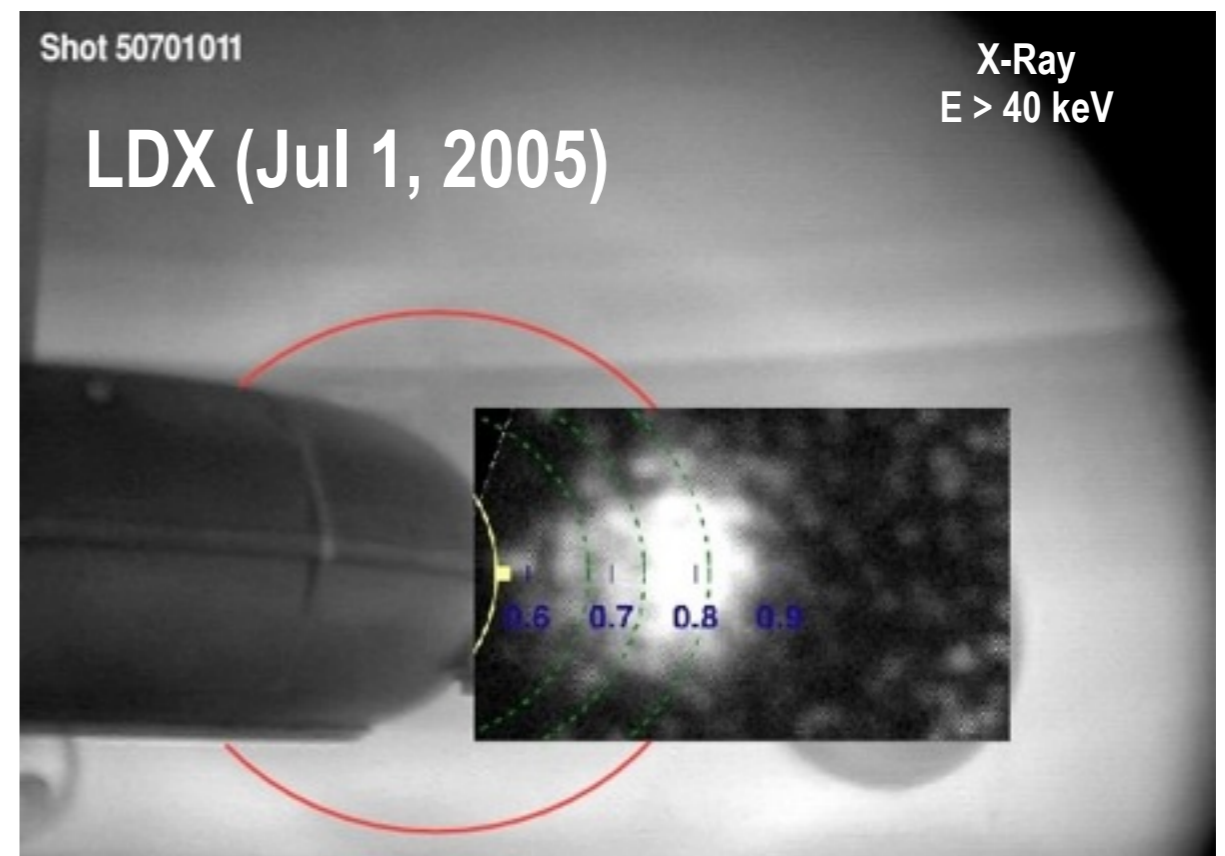
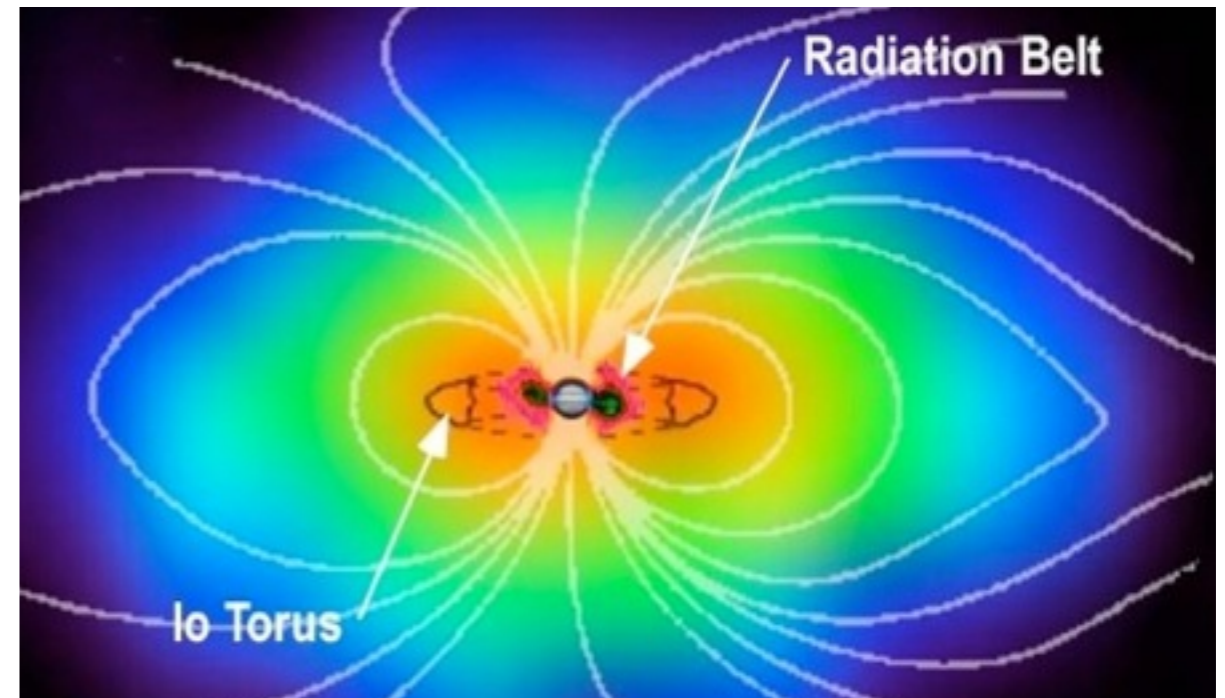
Discovered New 3rd Radiation Belt (2 MeV e^-) then annihilated by passage of interplanetary shock
ScienceExpress, Baker, *et al.*, 28 Feb 2013

Levitated dipole can achieve $> 50\%$ beta

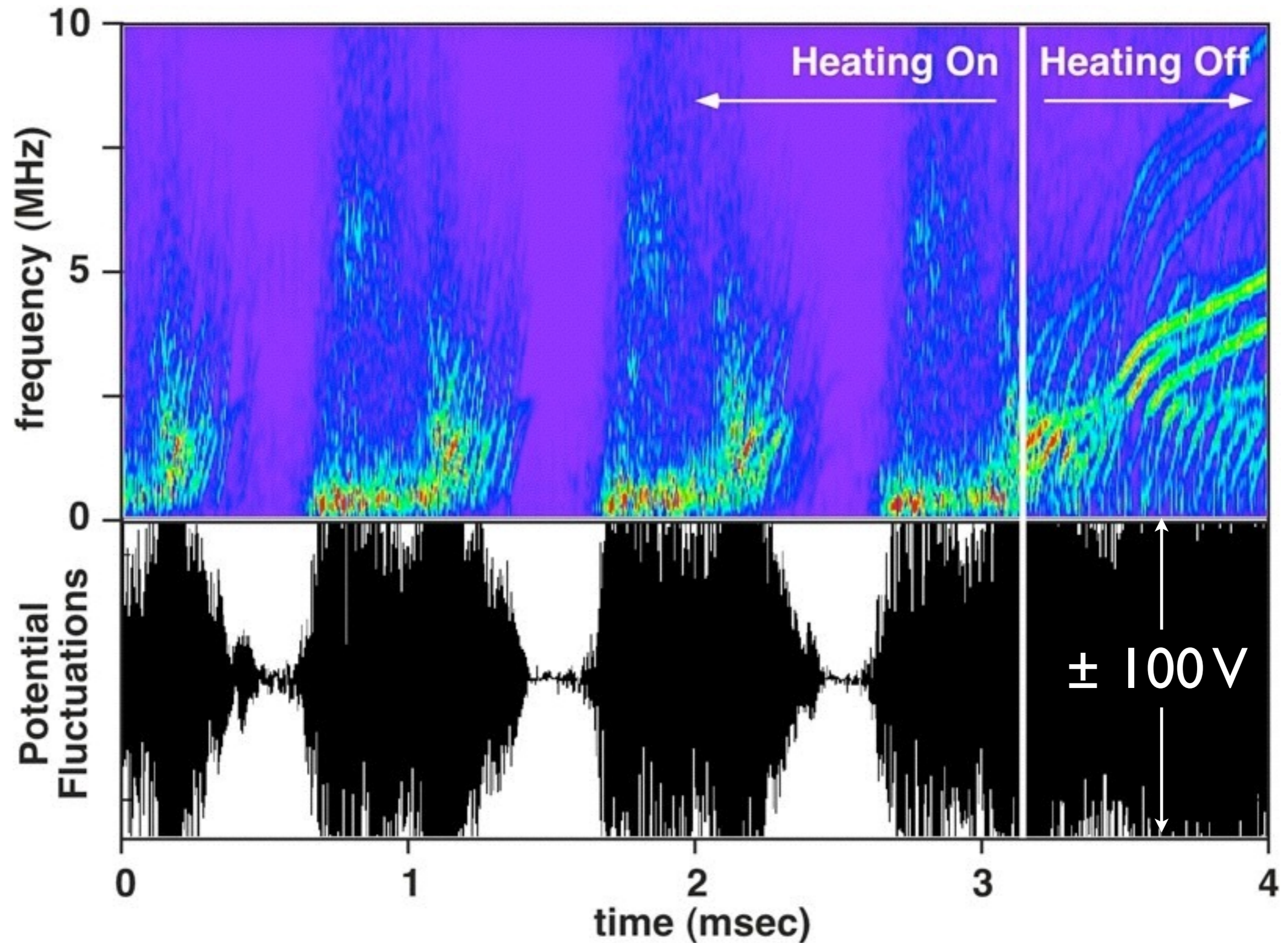
The natural high beta in planetary magnetospheres can be achieved in the laboratory. Steady-state.

- Garnier, POP (1999) shows equilibria with $\beta > 100\%$ possible
- Garnier, POP (2006) reports peak beta 20% achieved
- Garnier, NF (2009) reports peak beta doubles with levitation
- ➔ Saitoh, JFE (2010) reports peak beta 70% achieved in RT-1

Cassini at Jupiter (Dec 30, 2000)



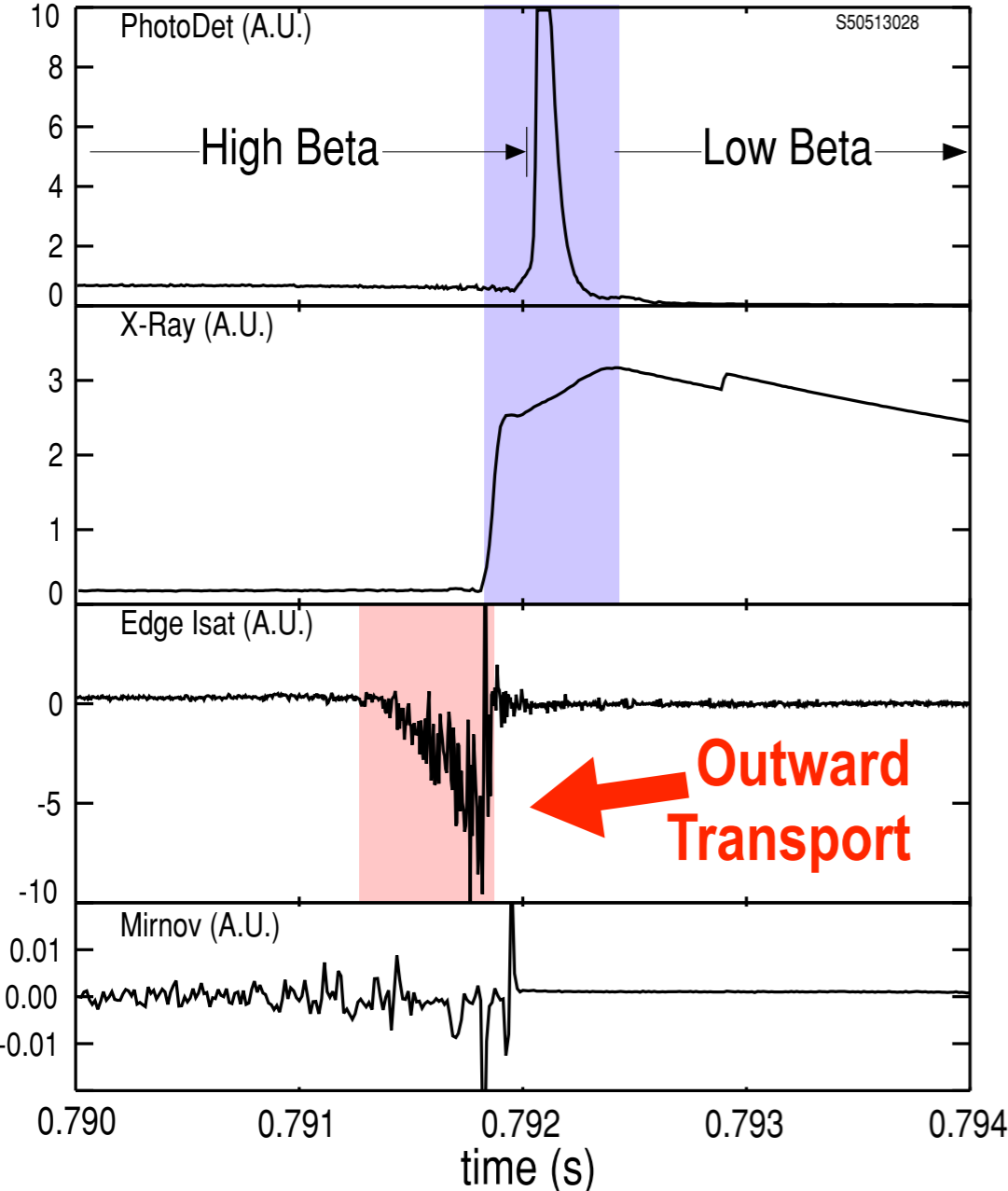
Drift-Resonant (Hot Electron) Interchange Instability



Kinetic Interchange Drift Resonance with High- β “Artificial Radiation Belt”

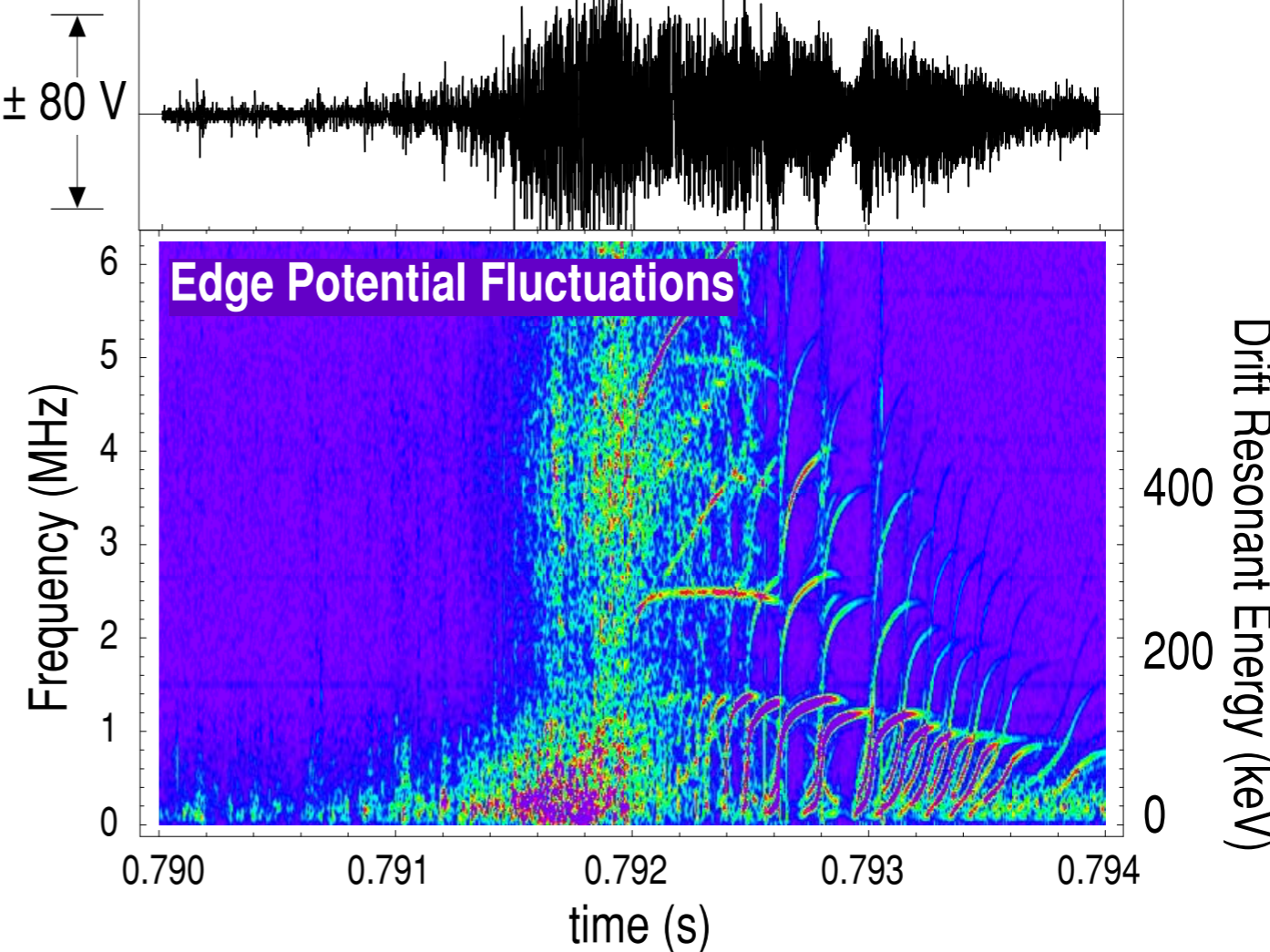
Fast drift-resonant instability resonates with fast electrons causing **rapid** radial transport...

Inward Transport

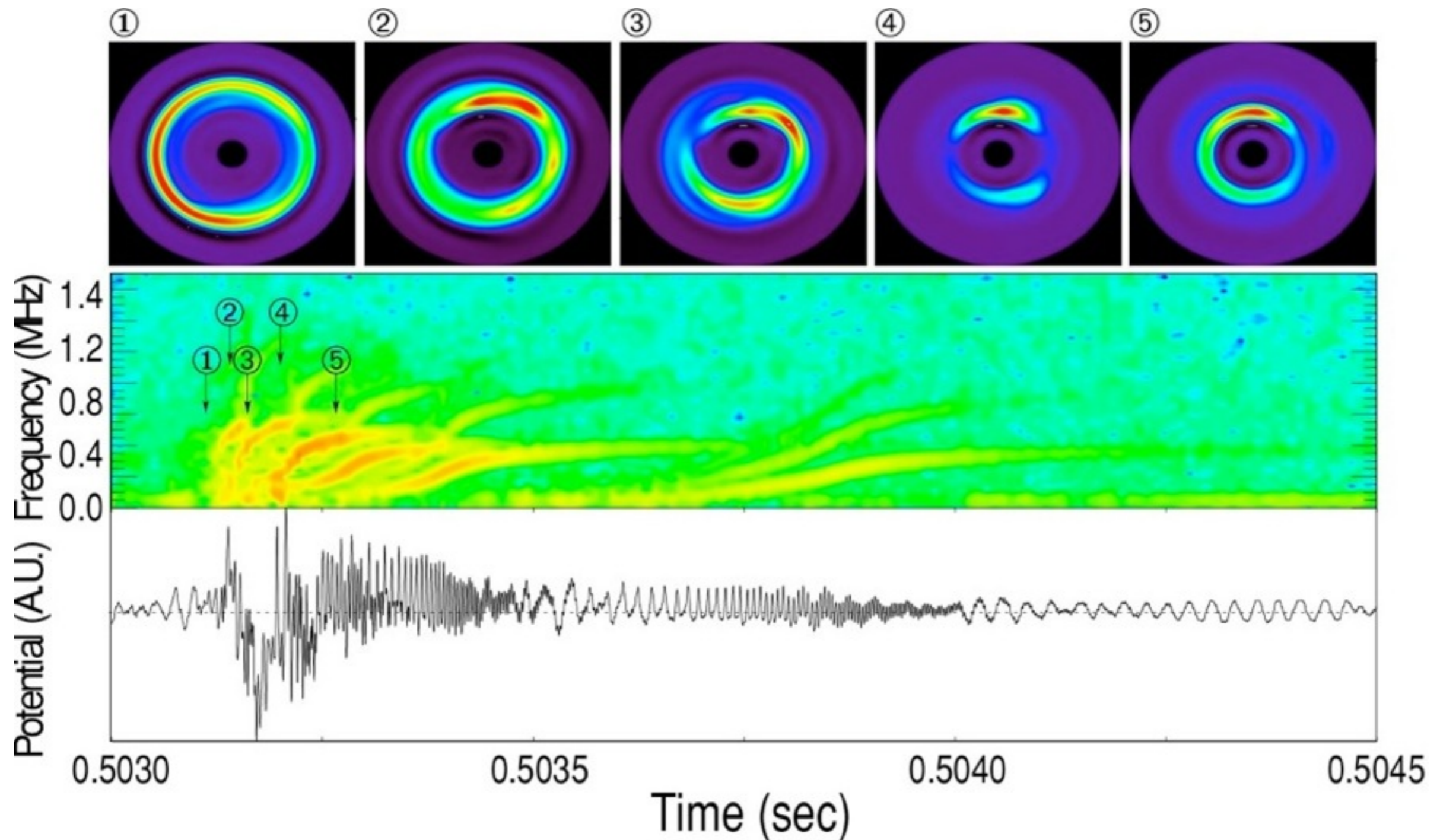
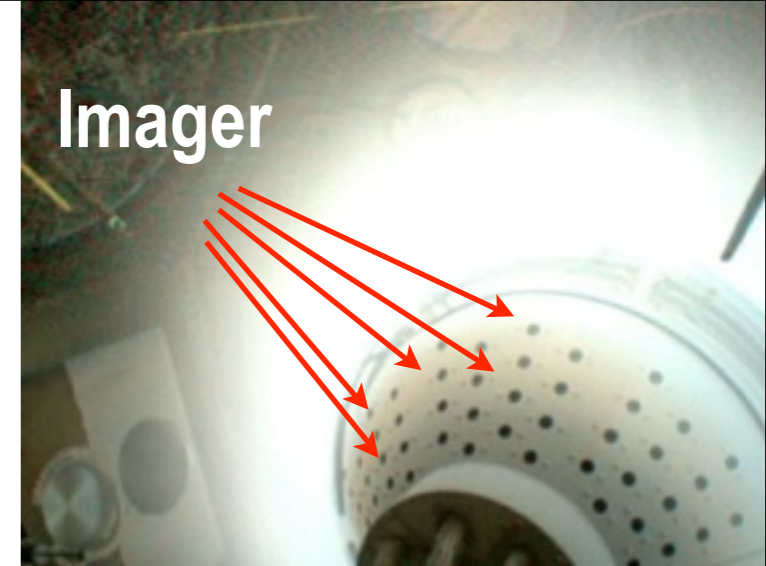


Outward Transport

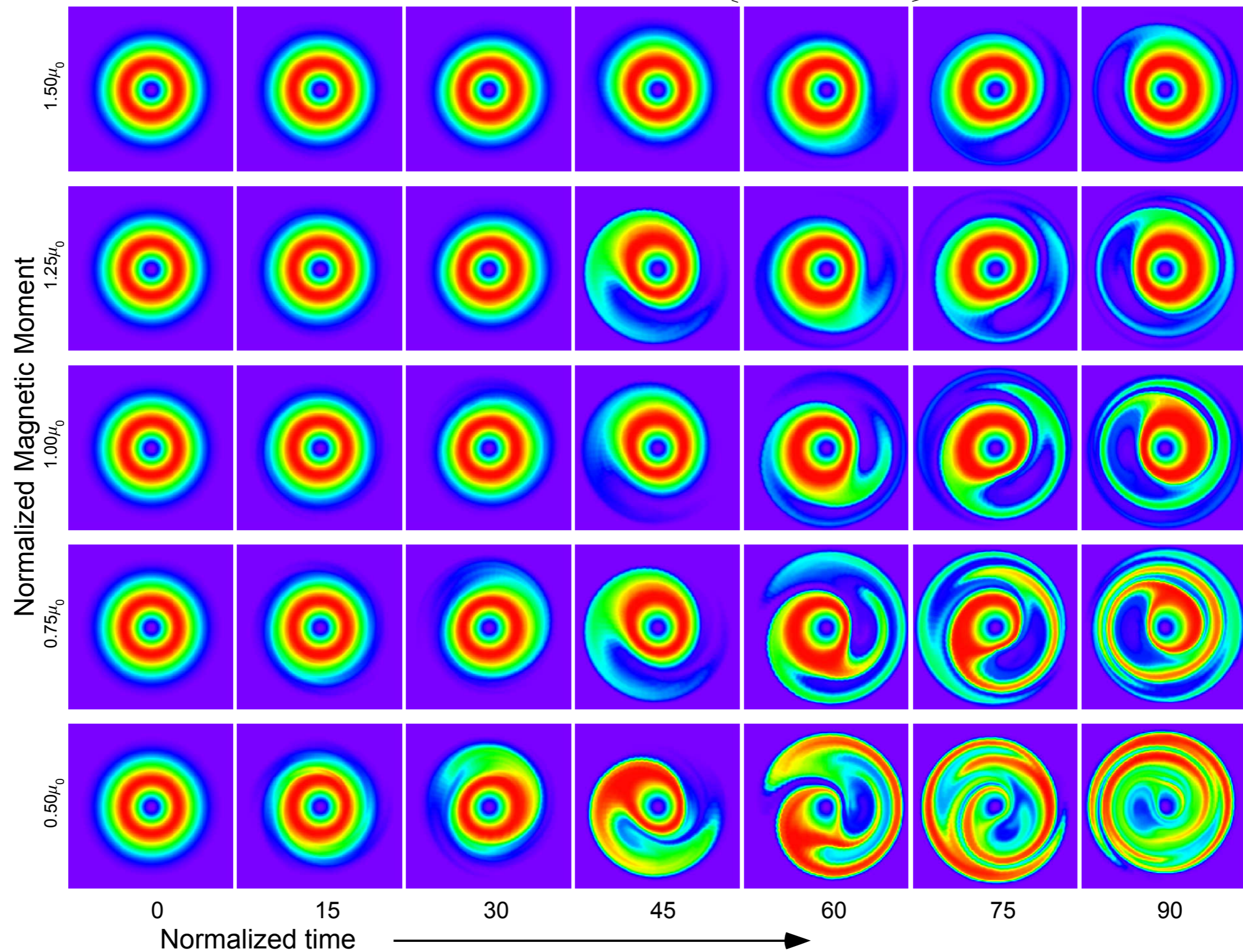
Chaotic Radial Transport Nonlinear Frequency Sweeping



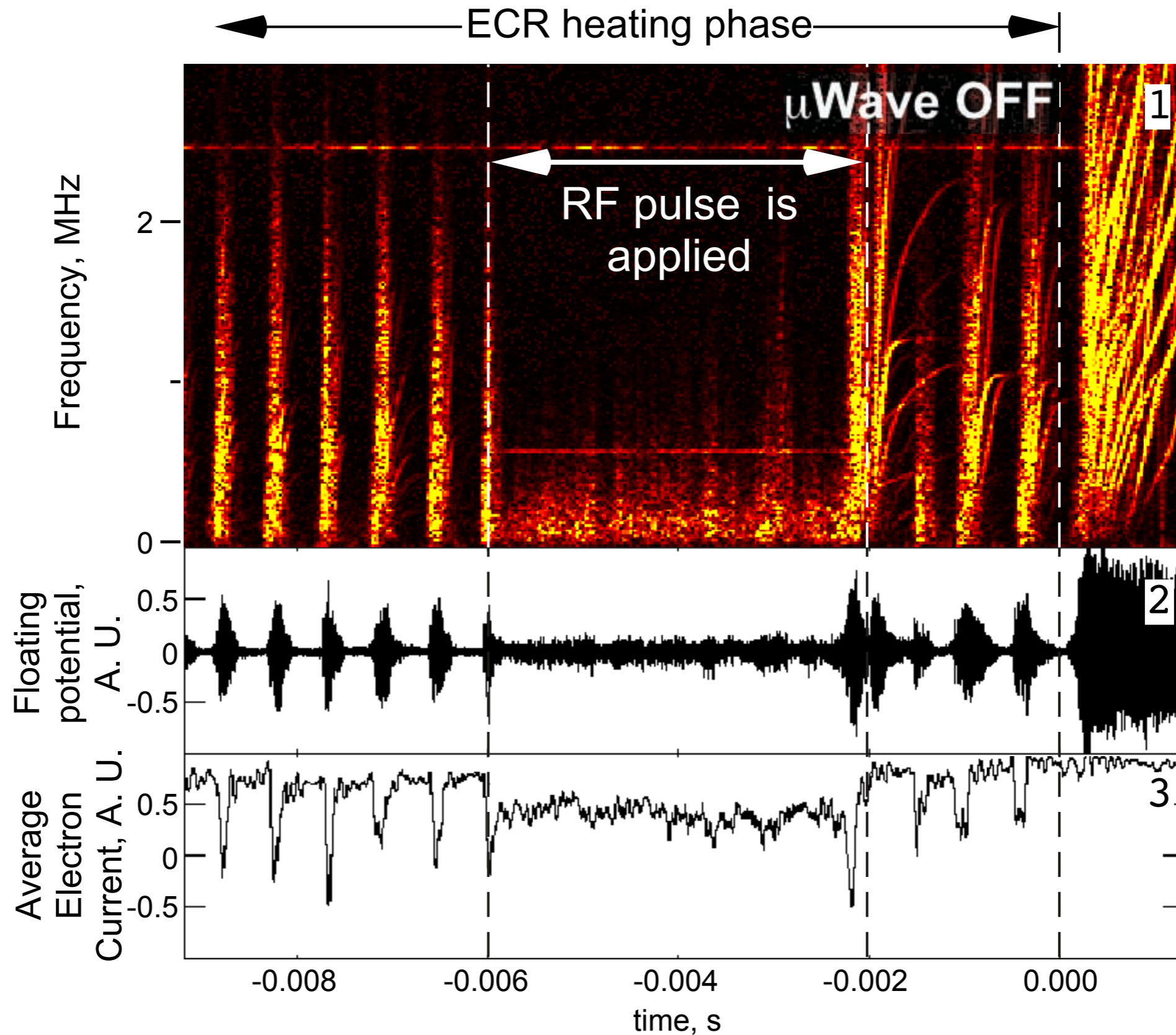
Polar Imager: Measuring **Inward** Drift-Resonant Transport due Gyrokinetic Interchange Instability



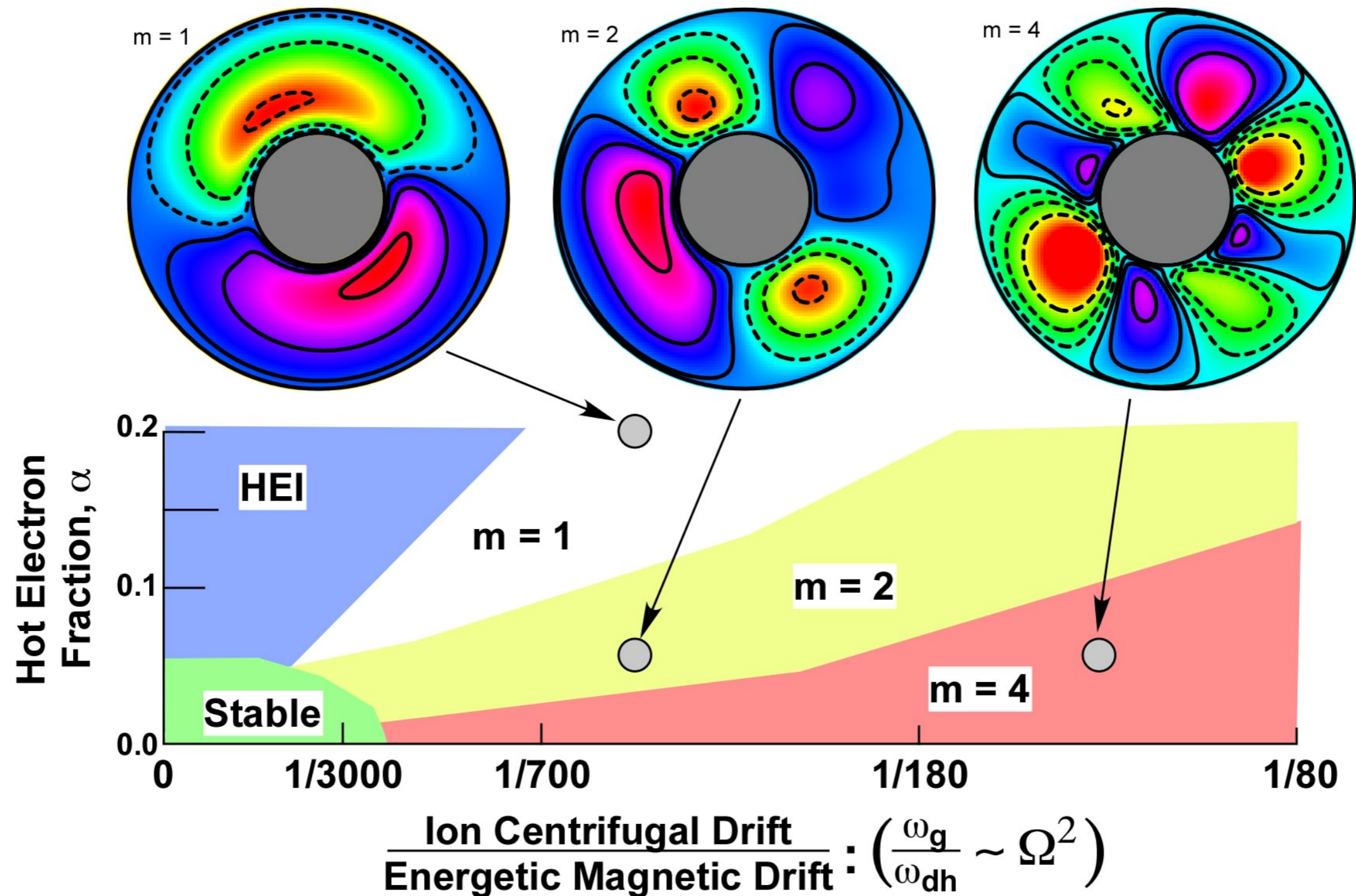
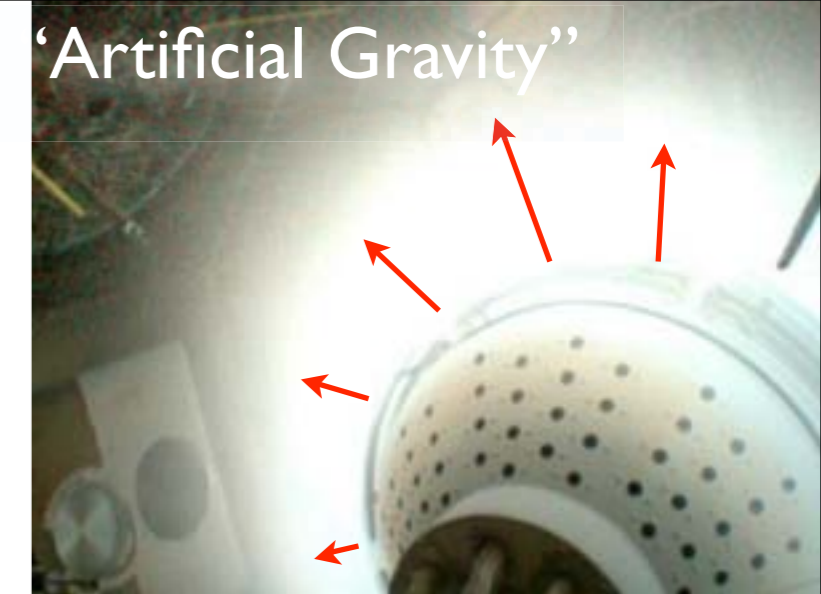
Drift Resonance $(\mu, J) \sim 1/L^2$



“Chorus” Injection Fills-in Phase-Space Holes

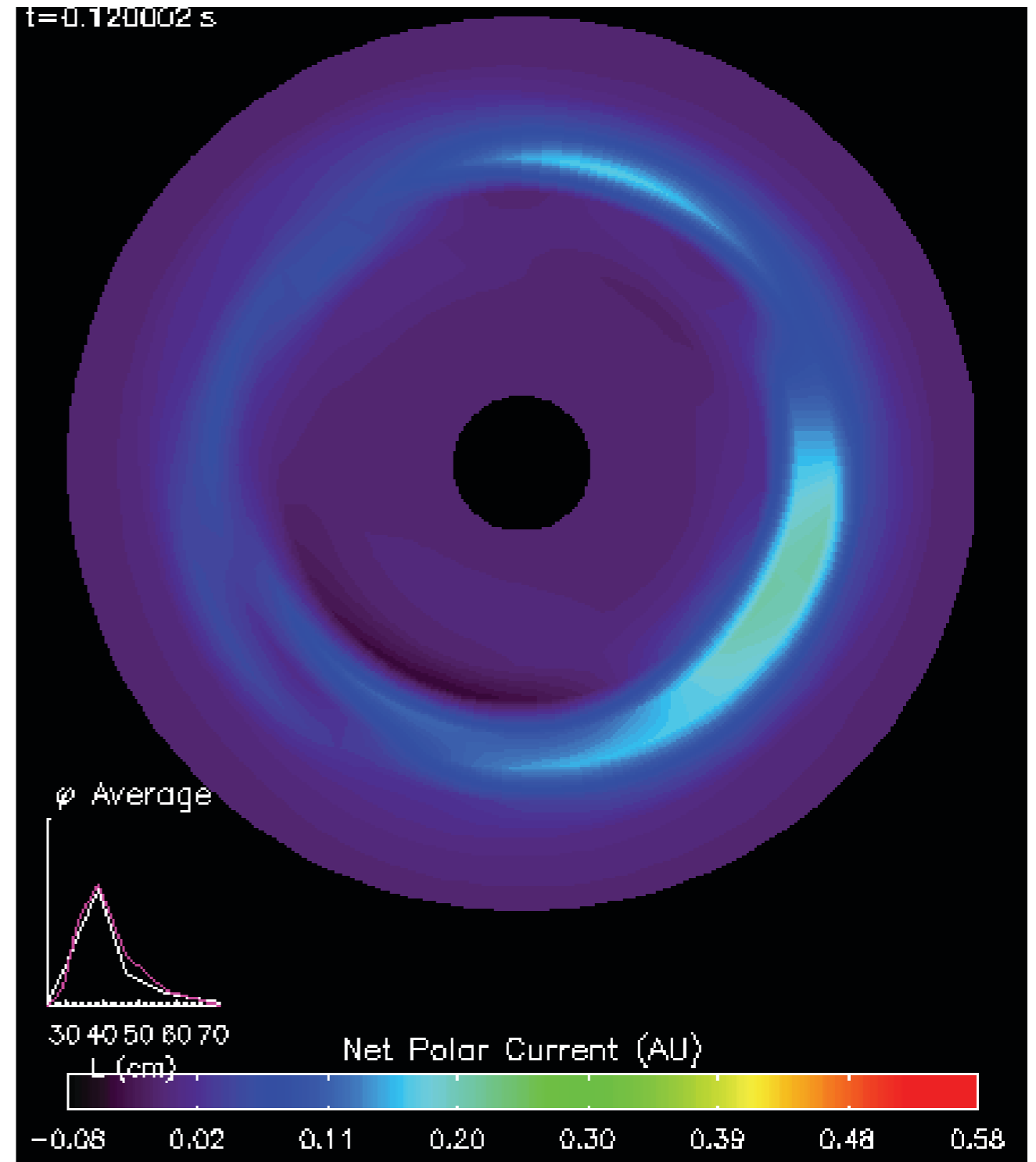


Relative Strength of Centrifugal and Curvature Drives Determine Nonlinear Mode Structure

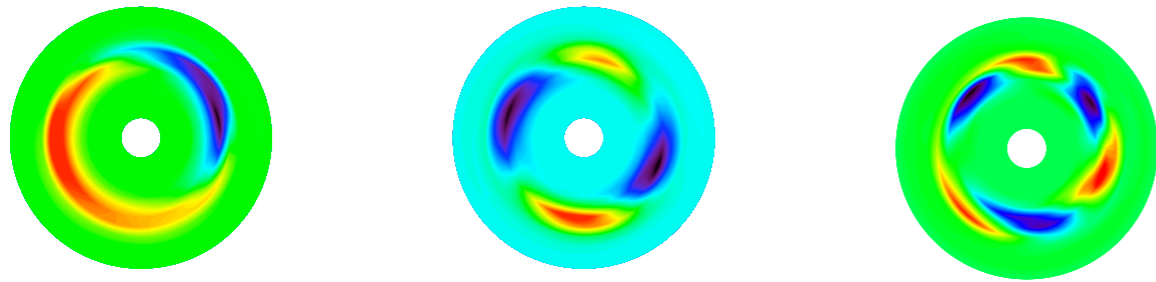


High Speed Imaging of Interchange Turbulence at 0.5 Mfps

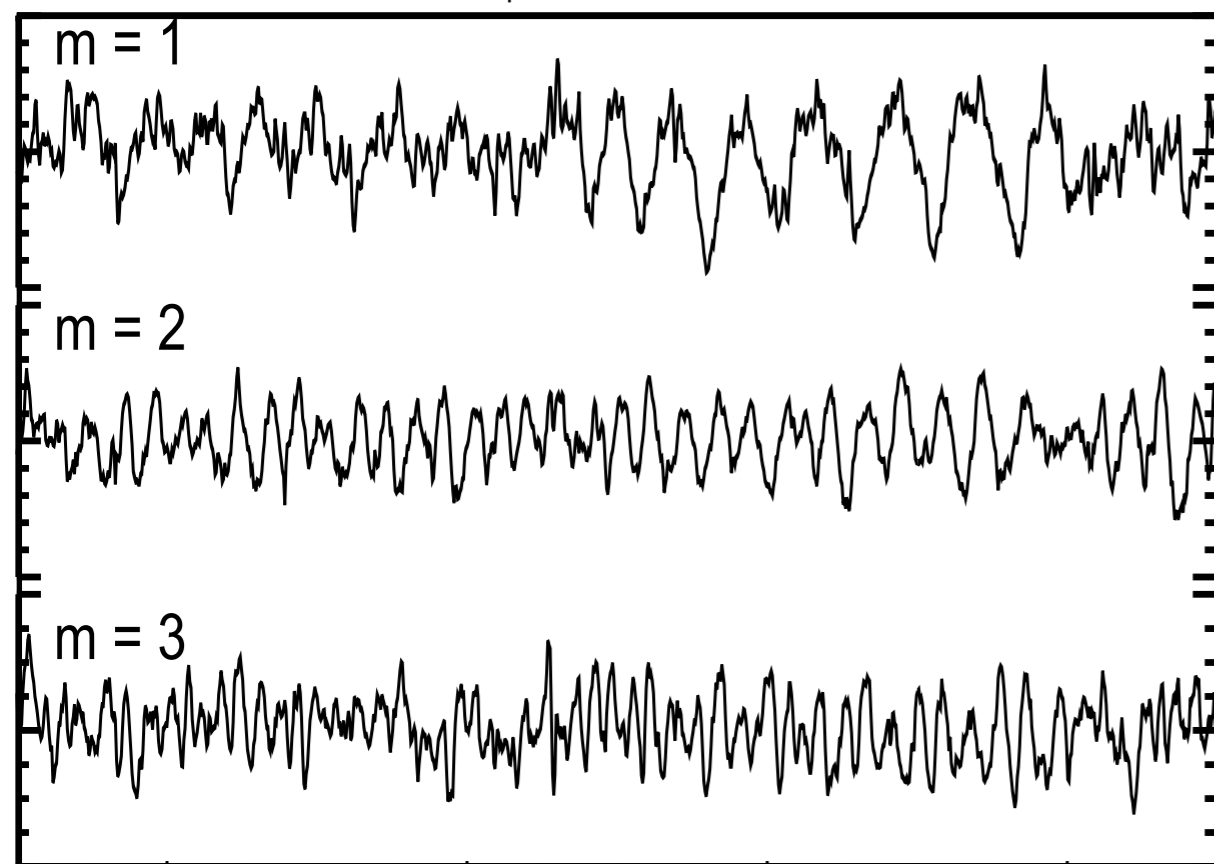
- Detectors biased to collect ion current
- Visualize turbulence
- Density fluctuations rotate in electron drift direction with random amplitude and phase modulations
- Compute turbulence cascade and compare with nonlinear simulations



Low-Frequency Turbulent Convection: Quantitative Verification of Particle Transport Models

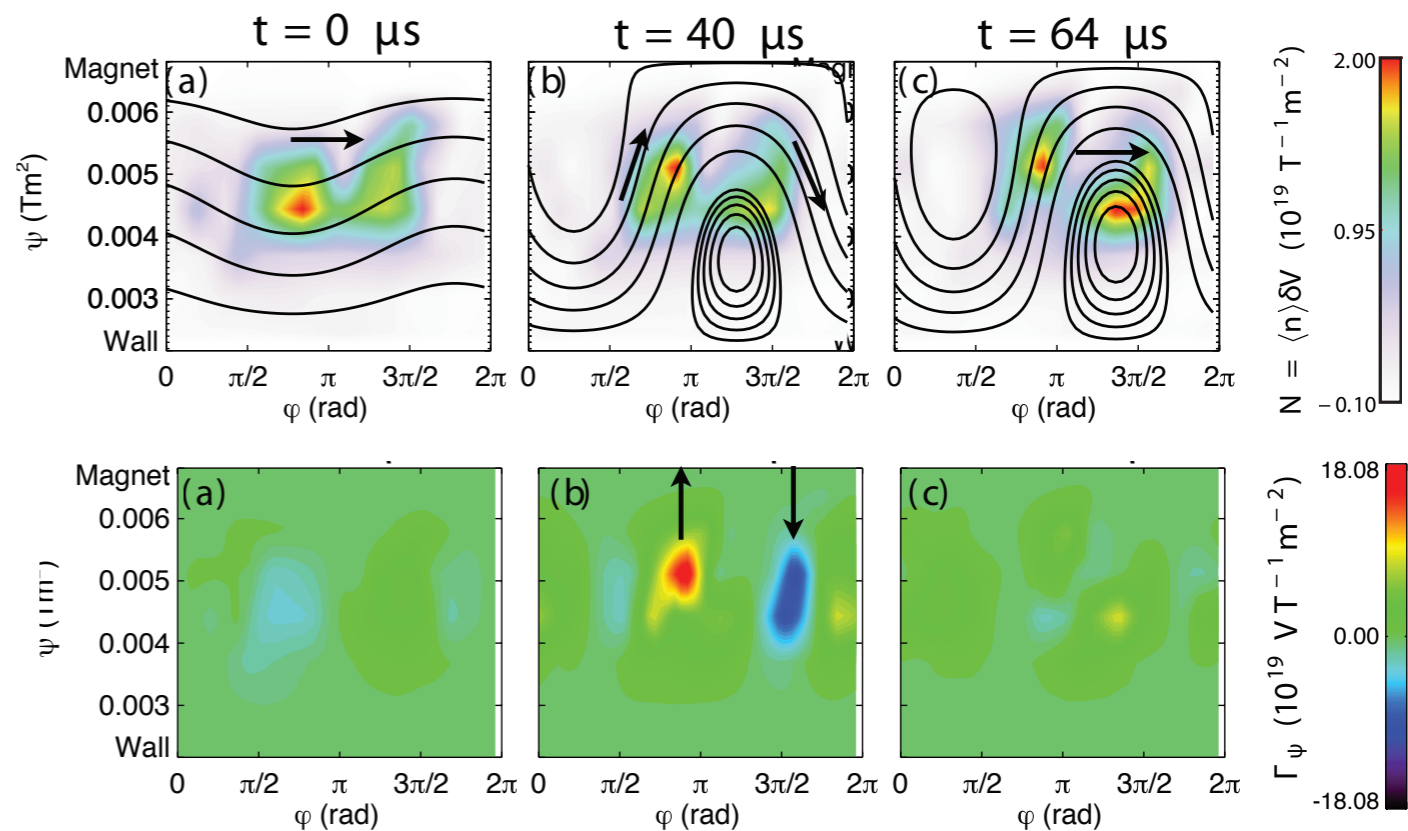


Interchange Transport of
“**Inward**” and “**Outward**” Moving
Plasma-Filled Flux Tubes



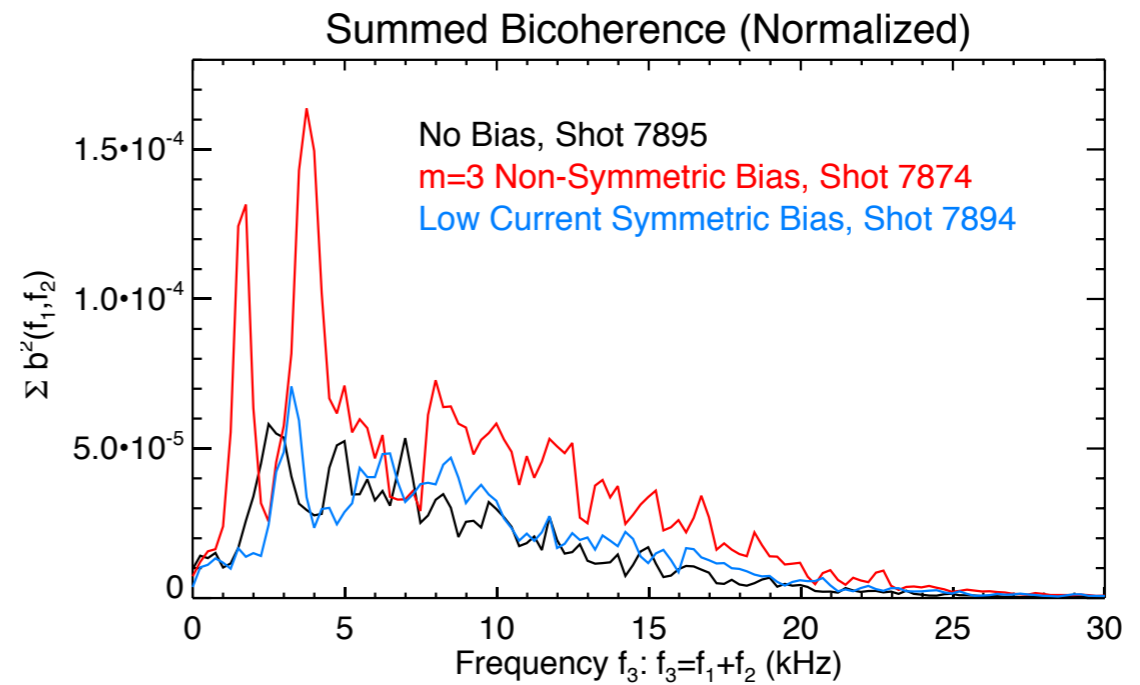
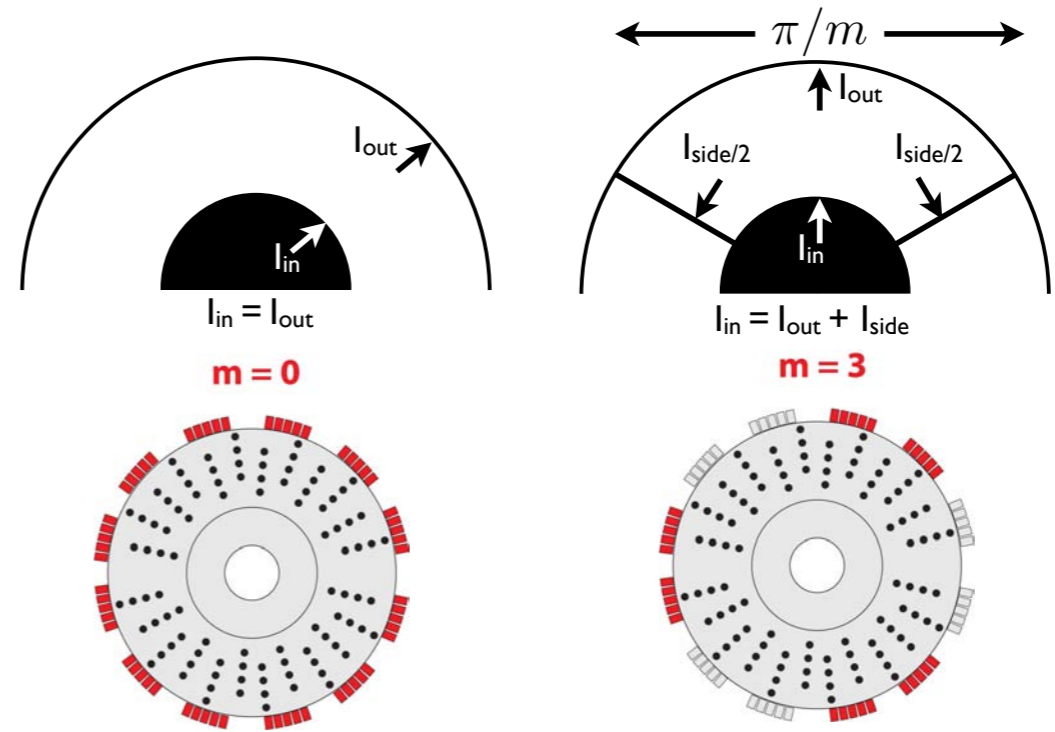
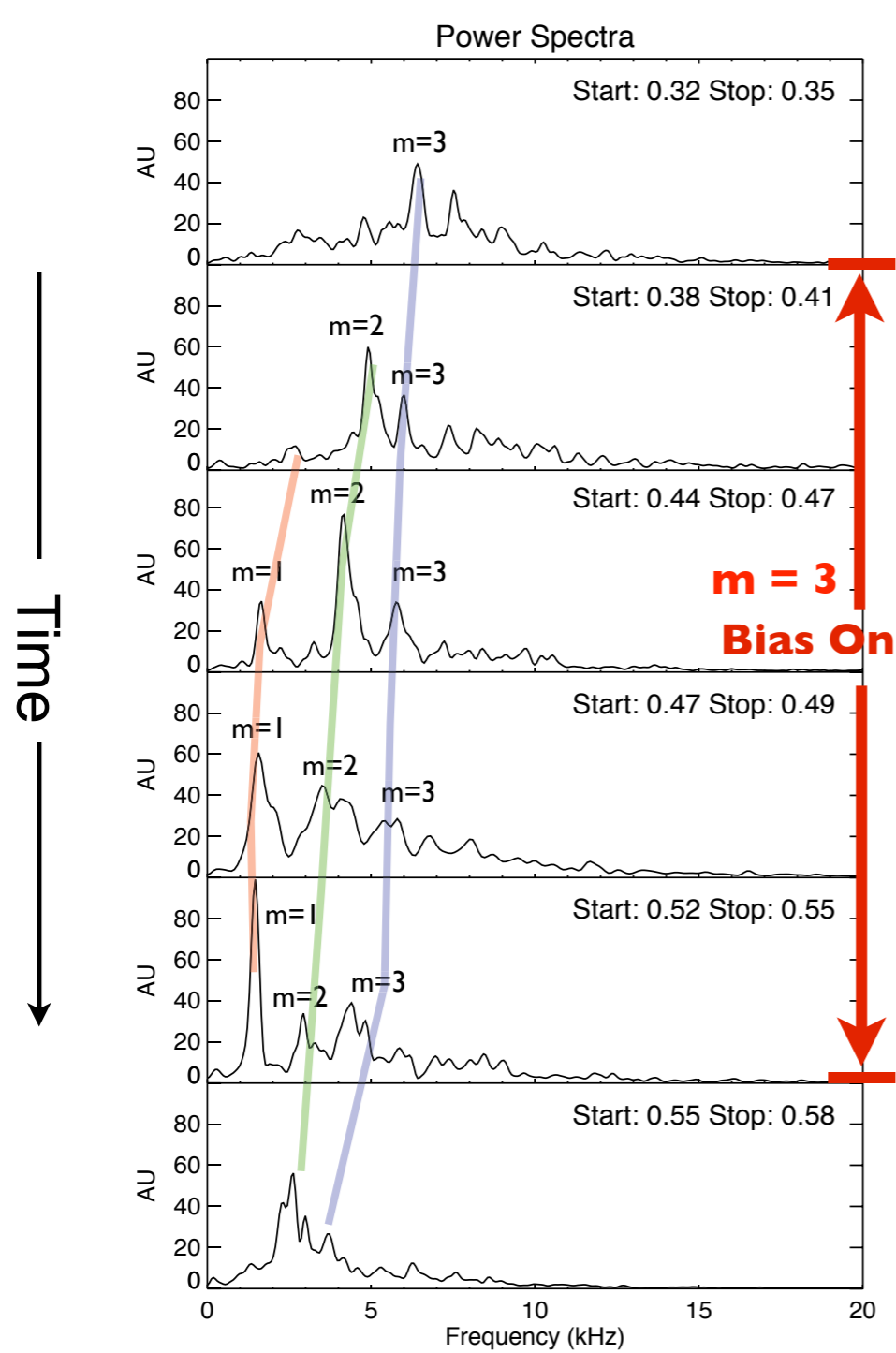
← 8 ms →

Convective Structures Dynamics



Chaotic Interaction between
Convective $E \times B$ Streamlines and
Plasma Density Perturbations

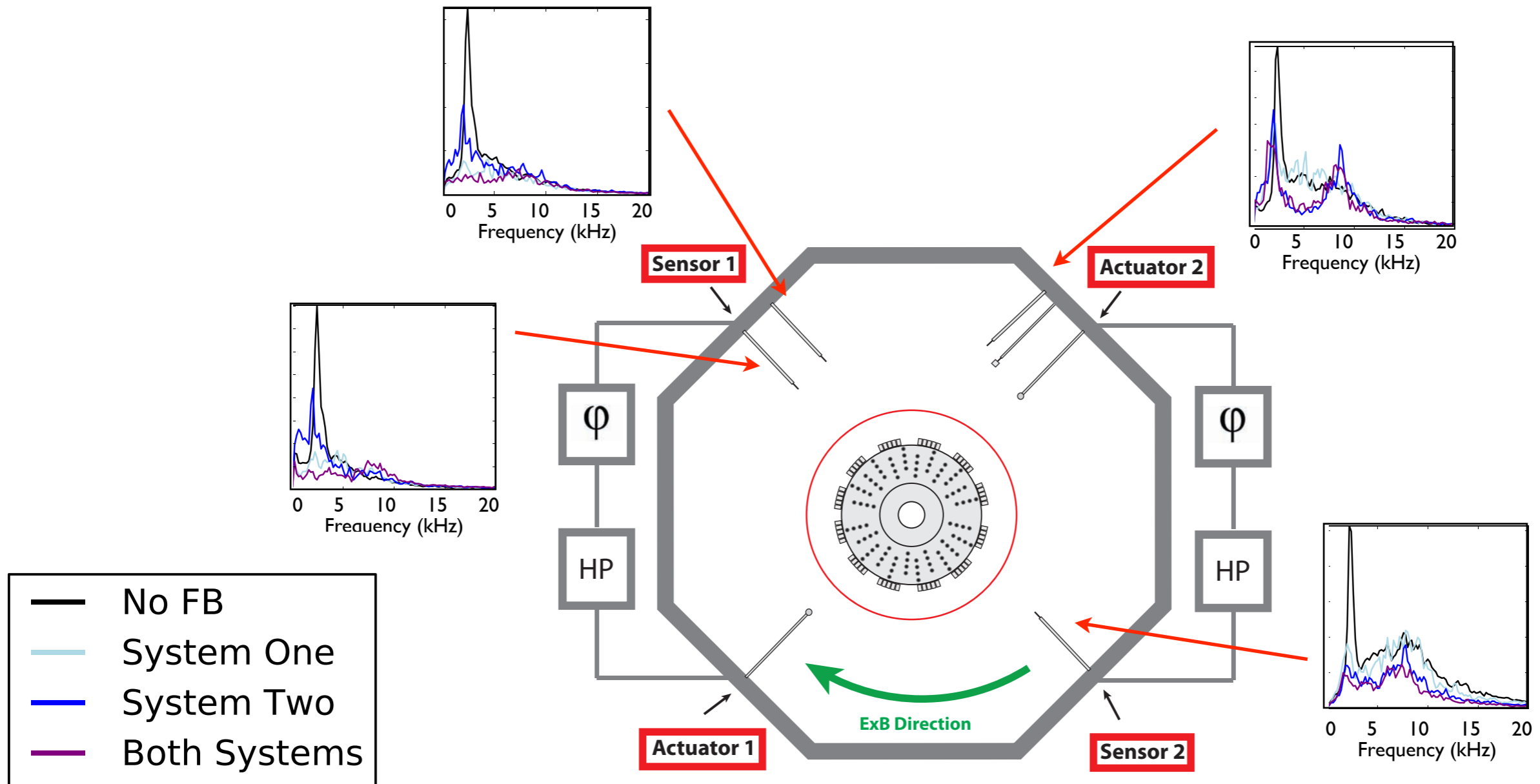
Symmetry Breaking and the 2D Inverse Energy Cascade.



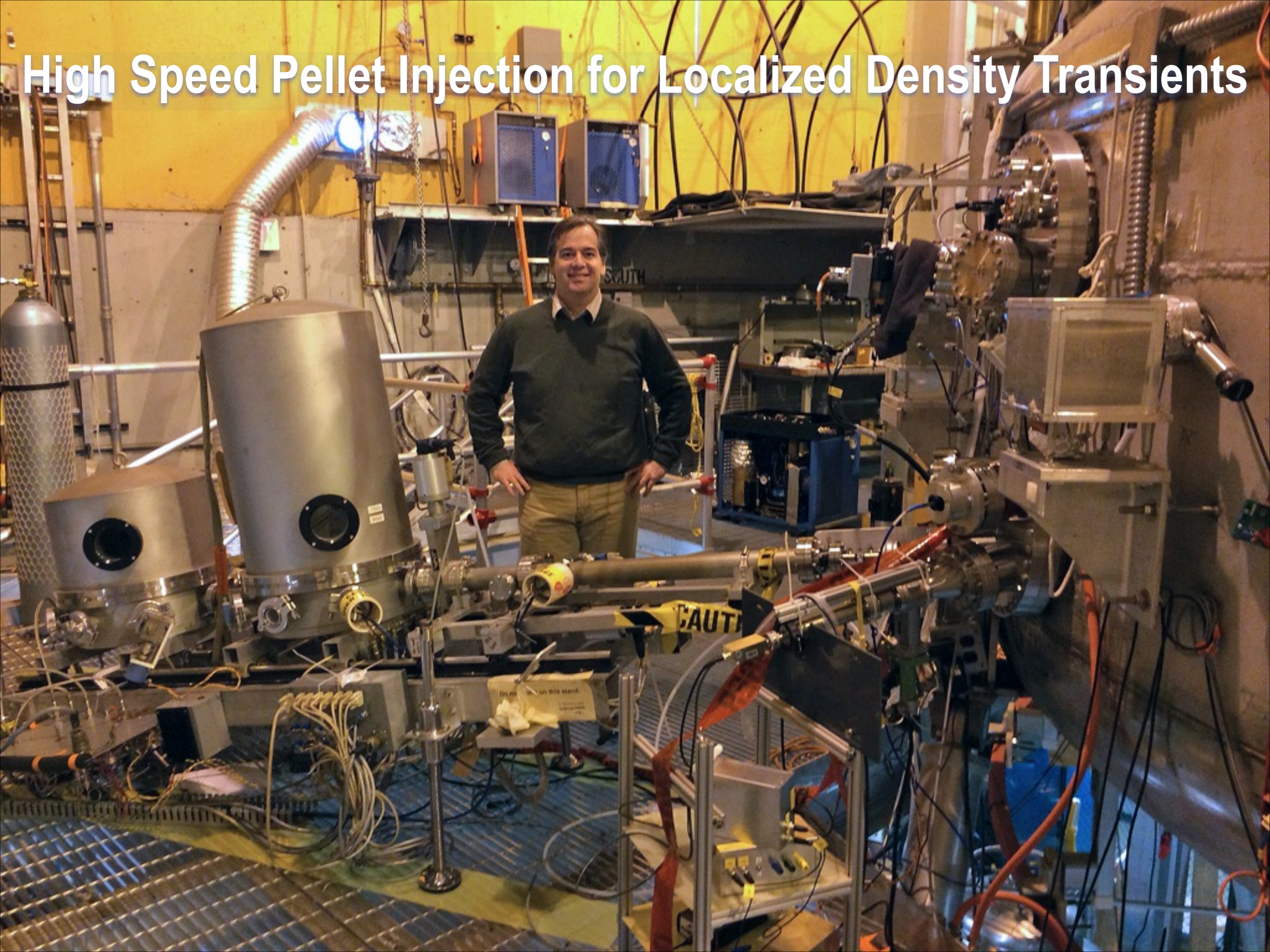
Current Injection for Dipole Turbulence Control

Problem: Turbulence decorrelates preventing global suppression

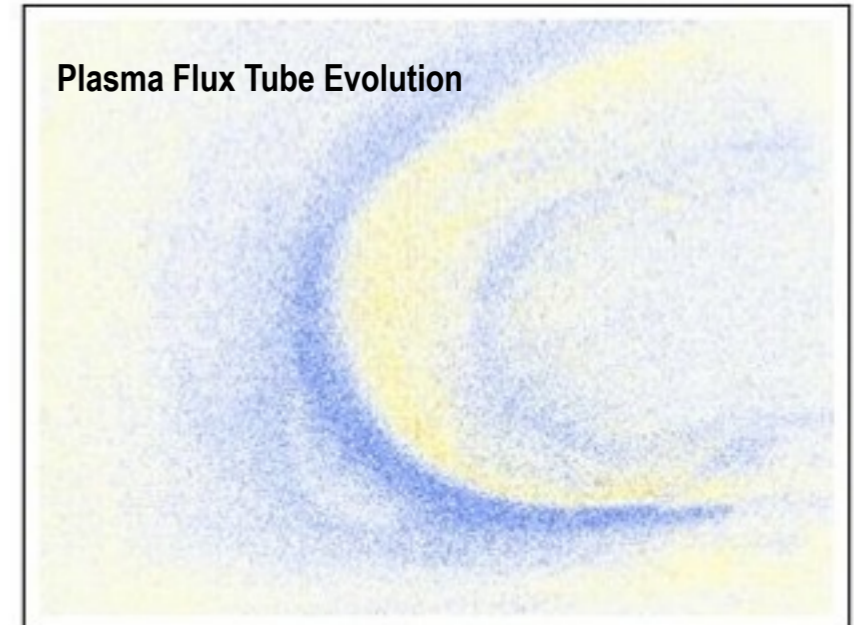
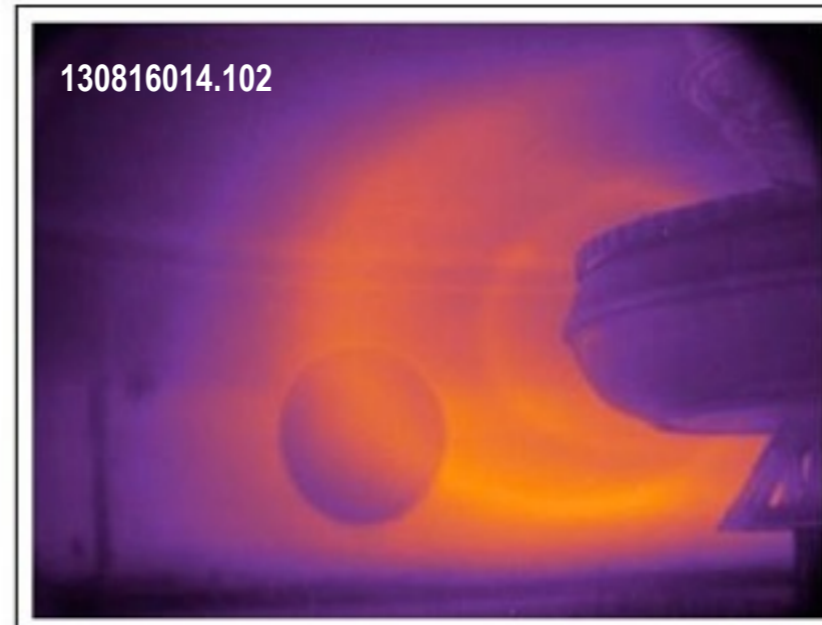
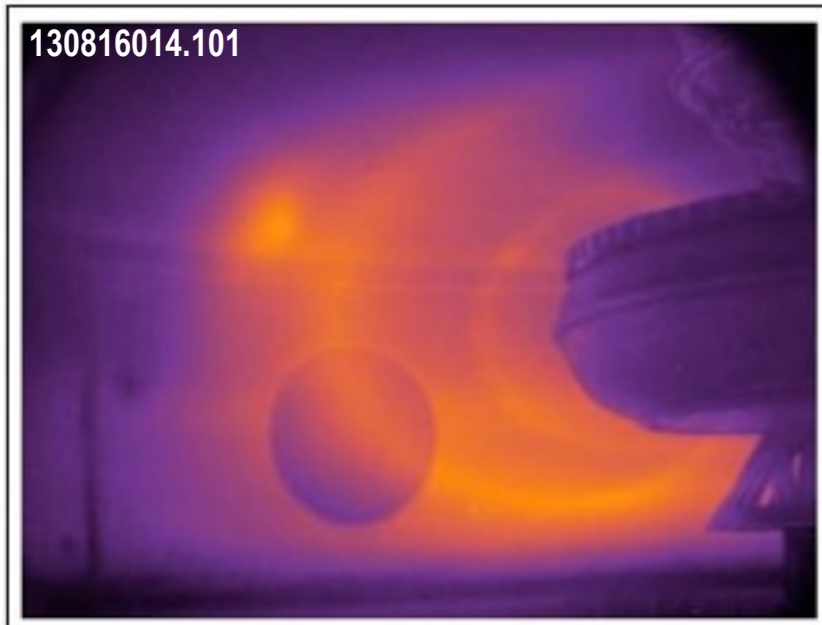
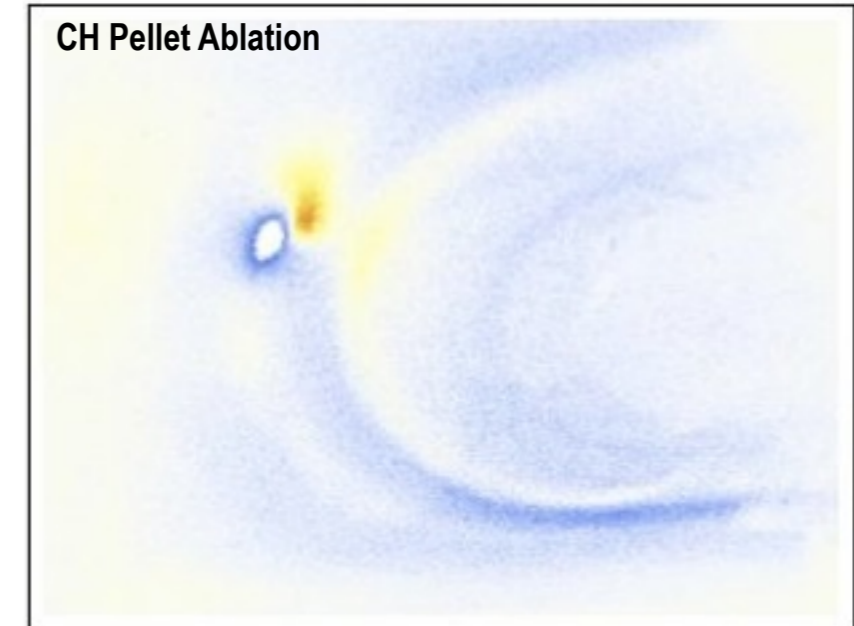
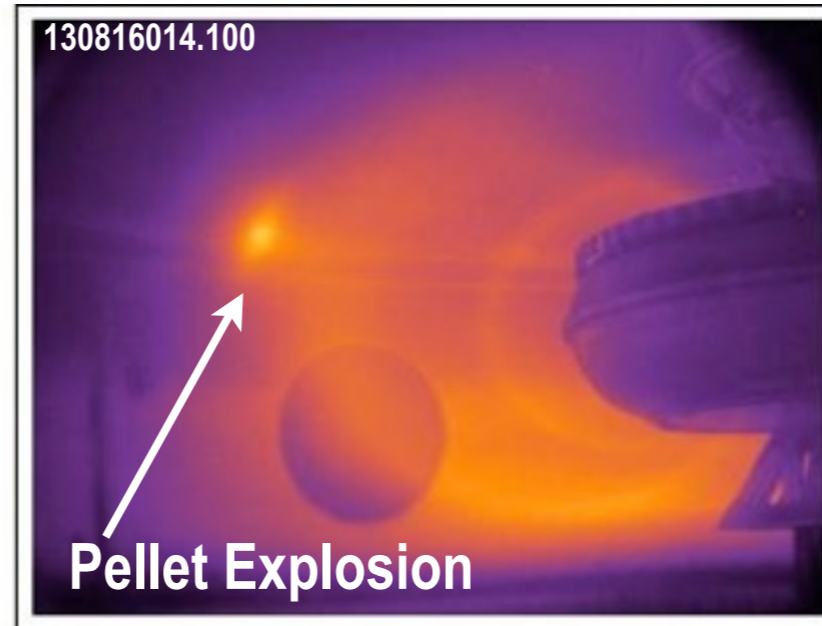
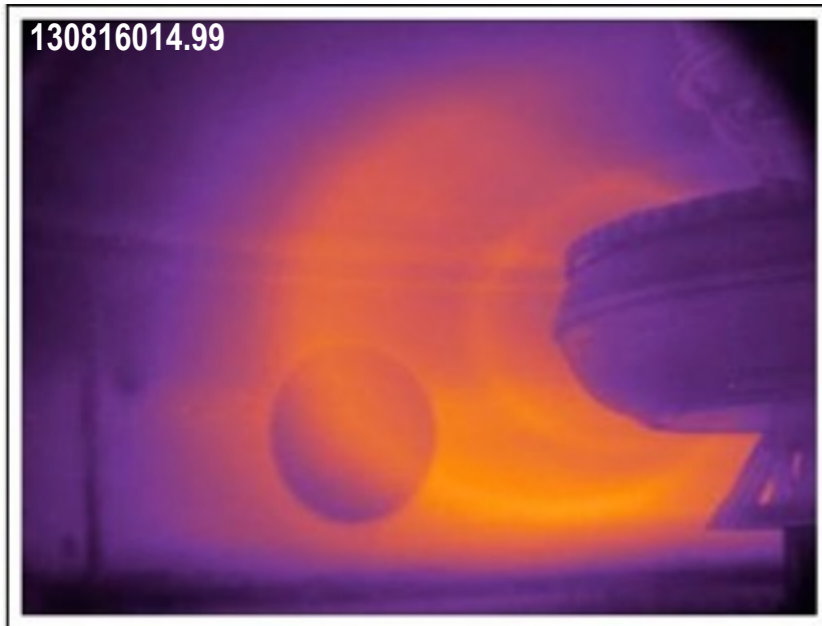
Solution: Apply multiple independent controllers



High Speed Pellet Injection for Localized Density Transients



Flux Tube Dynamics Following Pellet Release Experiments in Laboratory Magnetospheres

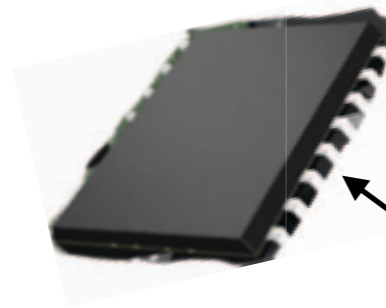


Low-cost "Smart-Probes" for Multiple-Point *in situ* Measurements



FRDM-KL05Z Development Board
With Arduino & USB Interfaces
3-axis accelerometer

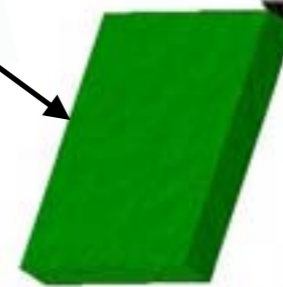
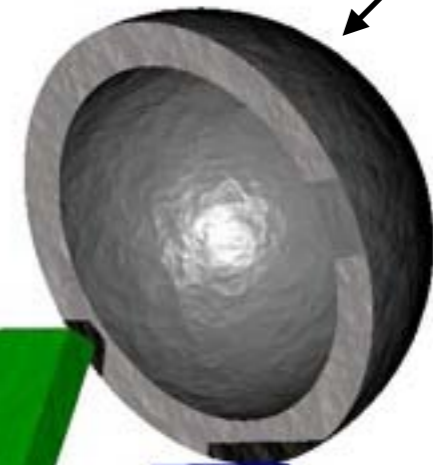
32 MB Flash Memory



KL05 MCU



Smart Probe Enclosure



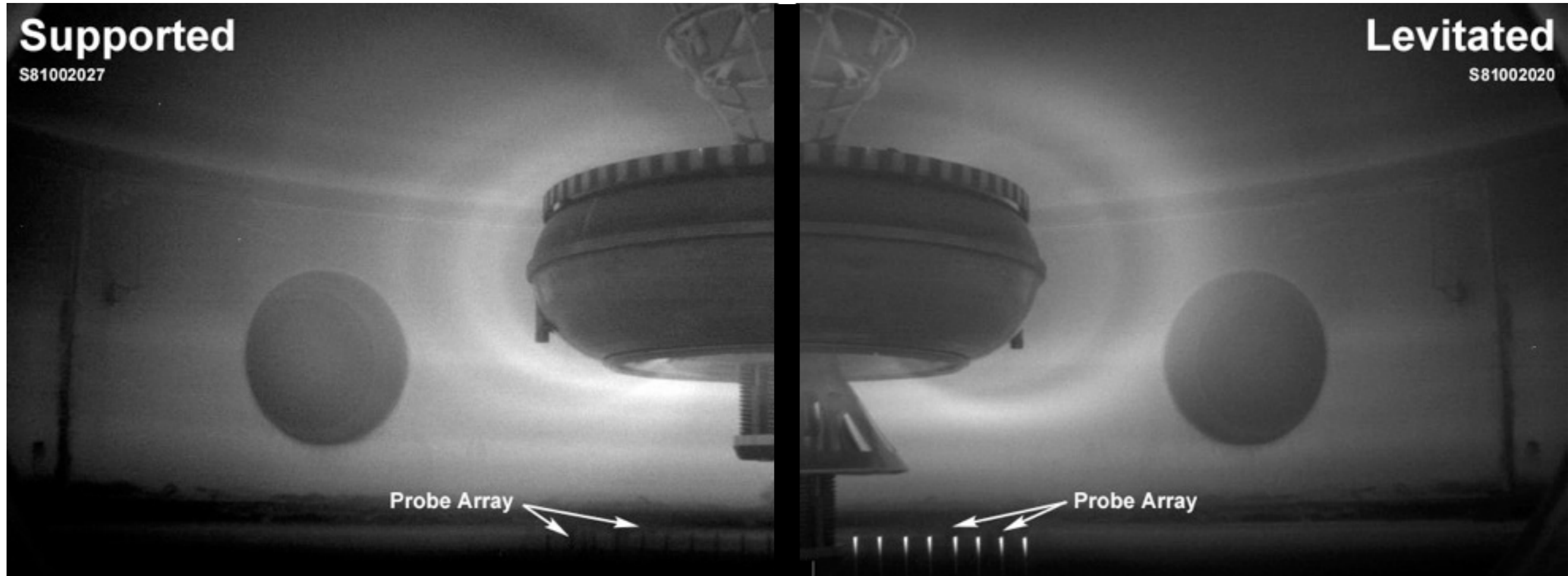
Battery Power



10 mm Dia

World's Largest Lab Magnetosphere

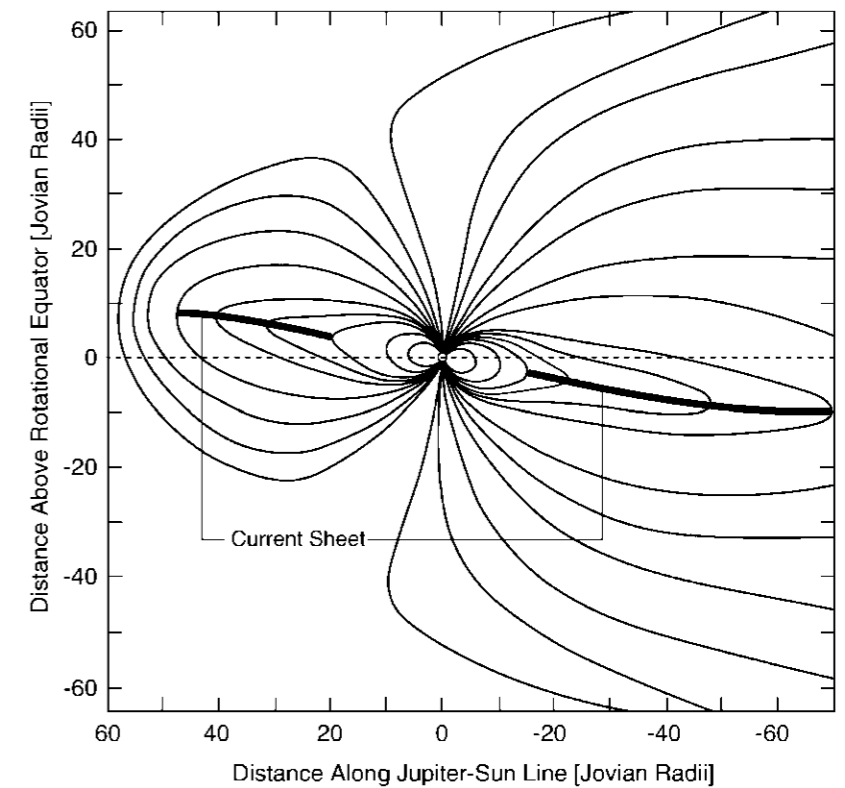
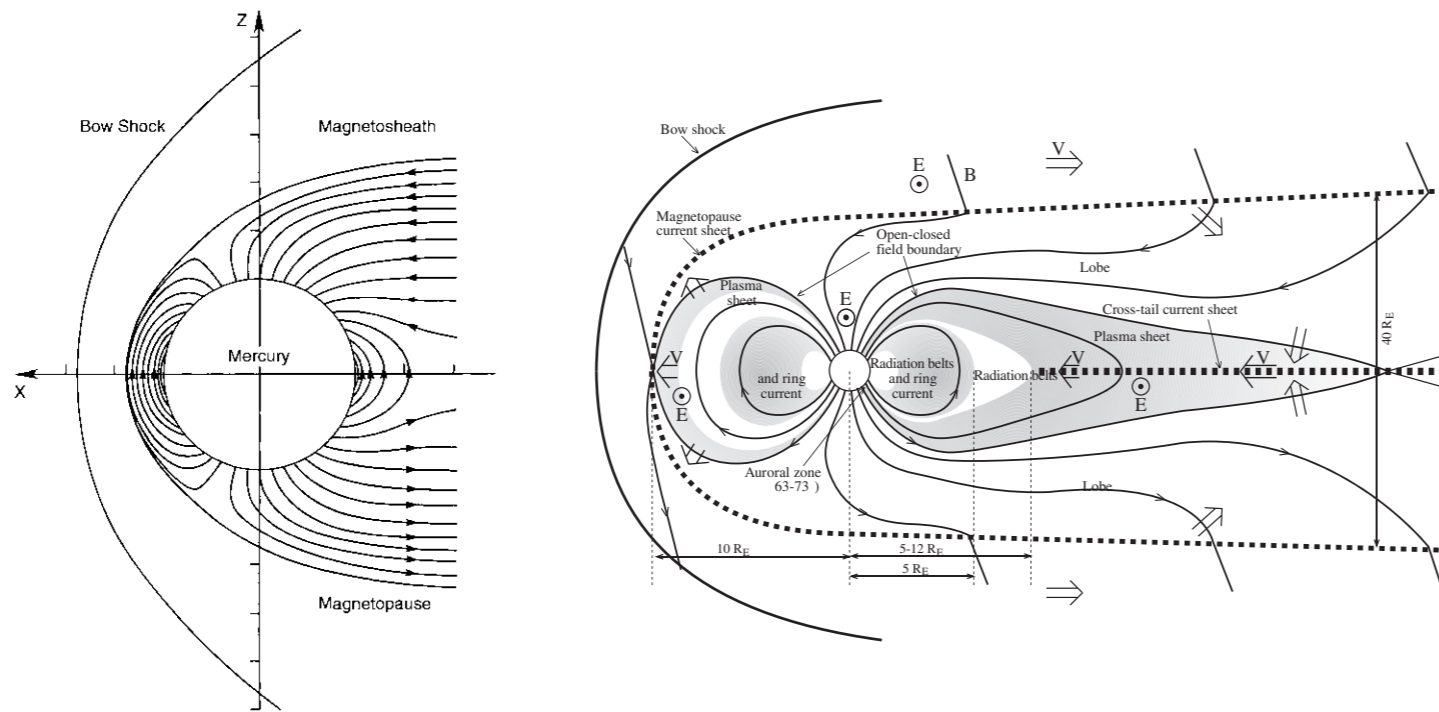
5 m



Size matters:

At larger size, trapped particle energy, intensity of “artificial radiation belt”, and plasma density significantly increase

High Density and Large Size are required for Controlled Investigations of Alfvén Wave Dynamics



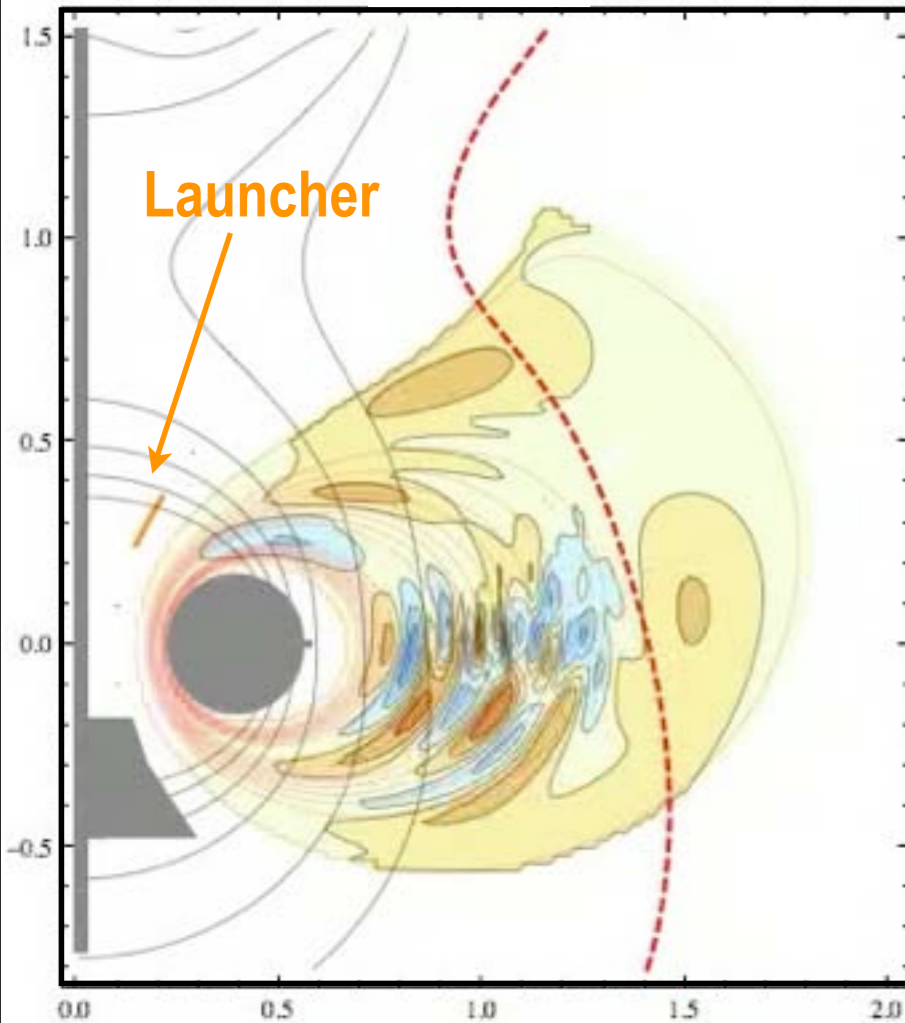
$$\frac{V_A}{L} \sim f_A \ll f_{ci} \rightarrow \frac{c/\omega_{pi}}{L} \ll 1$$

	Mercury	Earth	Jupiter
Size	2 R	10 R	100 R
Density (c / ω)	0.1	0.003	0.00001
Comments	V	Alfvén Resonances	Propagating Alfvén

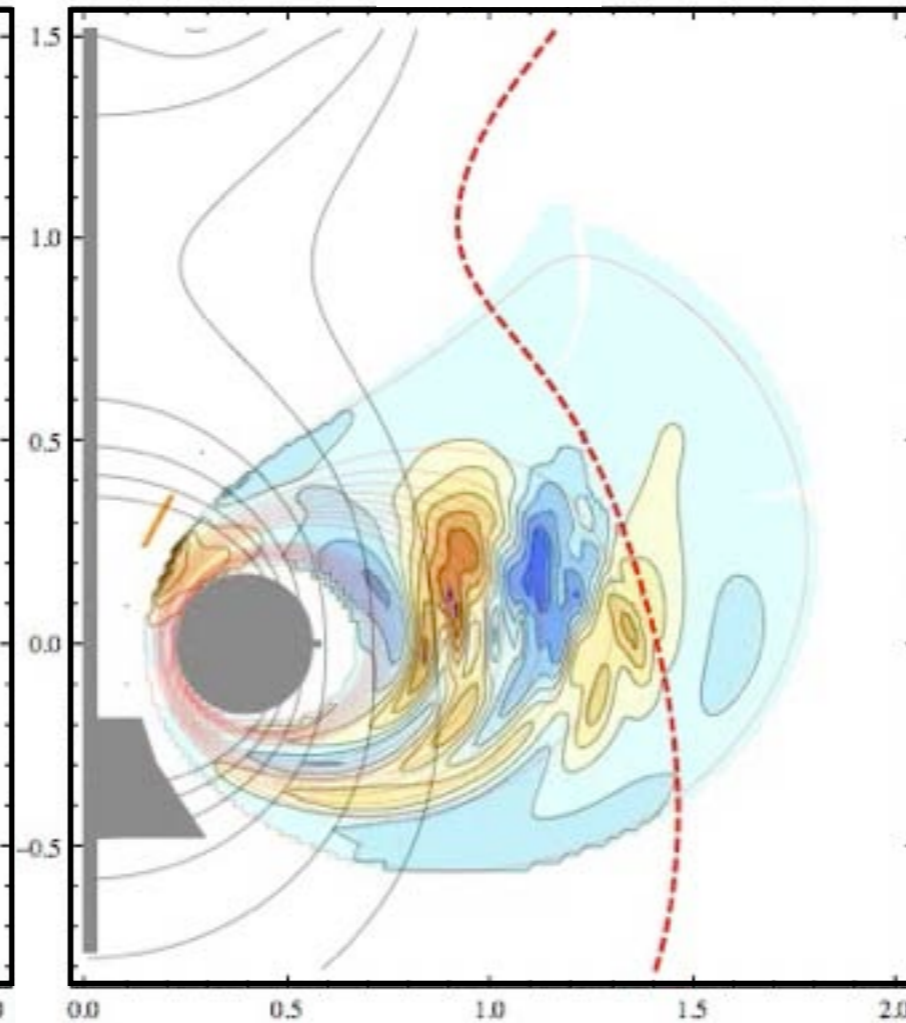
Alfvén Wave Excitation in LDX: Opportunity for a Many Important Experiments

- Alfvén Wave Spectroscopy and Resonances
- Toroidal-Poloidal Polarization Coupling
- Alfvén Wave interactions with Radiation Belt Particles
- Ion Cyclotron Resonance and FLR

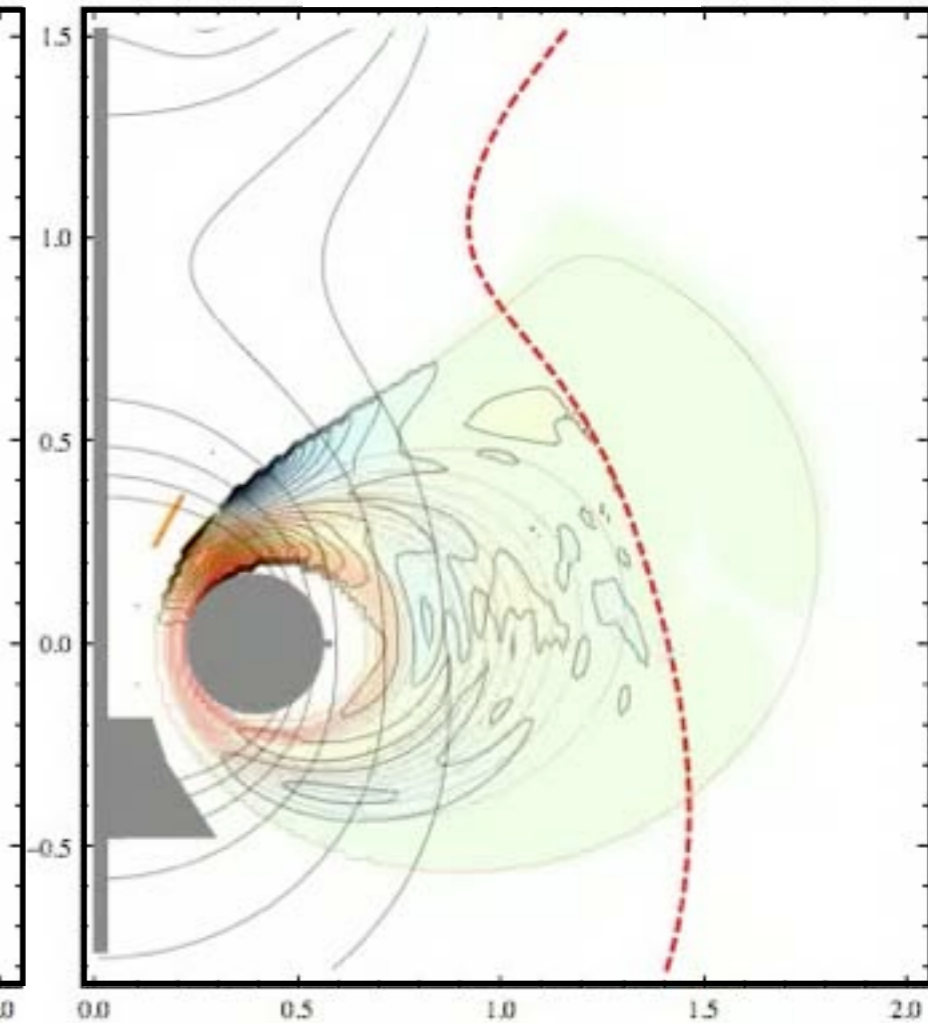
Toroidal



Poloidal



Compressional



Example: 200 kHz $m = 2$ Polar Launcher

NASA's early effort in Laboratory Testing and Validation can be Significantly Advanced with Modern Modeling and Diagnostics



NASA Glenn #5 (1966)



A Large Space Chamber Could be Filled with a Laboratory Magnetosphere



Space Power Facility (SPF)

Plum Brook Facility at Sandusky
World's Largest Vacuum Vessel



Laboratory Magnetospheres are Unique Opportunities for Controlled Space Physics Experiments

- Laboratory magnetospheres are facilities for **conducting controlled tests** of space-weather models in relevant magnetic geometry and for **exploring** magnetospheric phenomena by **controlling the injection of heat, particles, and perturbations**
- **Very large plasmas** can be produced in the laboratory, continuously, with low power and great flexibility. **Verification and discovery** of critical plasma science.
- “Artificial radiation belt” dynamics and transport can be studied. Preliminary tests of radiation belt remediation underway.
- Larger laboratory magnetospheres significantly increase trapped particle energy, intensity of “artificial radiation belt”, and plasma density. Allowing controlled tests of **complex Alfvén wave interactions** in the magnetosphere.
- **Outlook:** We can build/operate the largest laboratory plasma on Earth